CHEMICAL REVIEWS

Review

pubs.acs.org/CR

Interplay of Chemistry and Dynamics in the Low-Mass Star Formation

Yuri Aikawa*

Department of Earth and Planetary Sciences, Kobe University, Kobe 657-8501, Japan

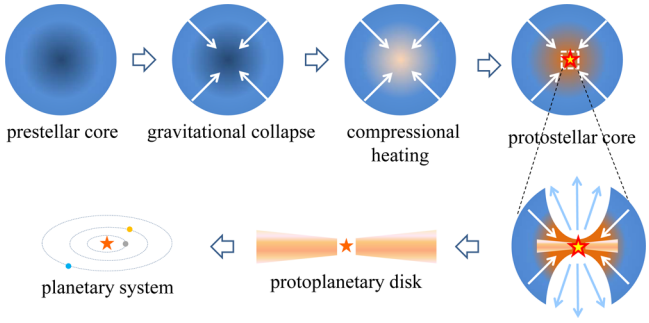

CONTENTS

1. INTRODUCTION

Interstellar space is filled with interstellar gas, which is composed of hydrogen (∼71% of mass), He (∼27%), and heavier elements (∼1%).[1−3] The gas contains small dust grains of silicate and carbonaceous material, which take up a significant fraction of the heavy elements, ranging from a few to several tens of percent depending on the elements.[4] Density and temperature of the interstellar gas vary spatially. For example, energetic UV radiation from massive stars can ionize hydrogen atoms and heat the gas to $\sim 10^4$ K, which is called HII region.[5] In regions relocated from such massive stars, interstellar radiation with <13.6 eV (ionization potential of hydrogen) is still available, and hydrogen is mainly in atomic form. In some regions, interstellar gas is accumulated so that the interstellar radiation is attenuated by dust grains, and the gas becomes molecular. They are called molecular clouds (Figure 1a). Due to the radiative cooling and lack of efficient heating source, the typical temperature of molecular clouds is as low as ∼10 K.[6] The number density of gas is $\sim 10^3$ molecular hydrogen per cubic centimeter (i.e., gas pressure $\sim 10^{-15}$ Torr) or higher, which is significantly low compared with the gas density in the vacuum chamber in laboratories on Earth but is relatively high in interstellar space.

Molecular clouds are a very unique chemical laboratory. Due to the low gas density, the collisional time scale among gas particles is as long as a few days, so that radicals and ion molecules, which would be promptly destroyed by reactions in laboratories on Earth, can be as abundant as $\geq 10^{-10}$ relative to H_2.[9] Although the abundances of 10^{-10} may sound low, it corresponds to a sufficient column density of the molecule to be detected by radio telescopes in many cases, thanks to the huge spatial scale and total mass of molecular clouds (see below). Spectroscopic survey of molecular lines have found various exotic species such as H_3^+, C_4H, and C_6^-,[10−12] as well as more familiar molecules such as H_2O, NH_3, and CH_3OH.[9] Assignments and confirmation of these observed lines have been done by many dedicated spectroscopic studies.[13,14]

Molecular clouds are important for astrophysics as well, since they are the formation site of stars and planets. In this paper we mainly consider the region of low-mass stars formation, where Sun-like stars are formed. Although the typical density of molecular clouds are as low as $\sim 10^3$ cm^{-3}, the gas extends over such a huge scale, 10−100 pc (1 pc is about 3.1×10^{16} m, which corresponds to about 2×10^5 times the distance between Earth and Sun), that the clouds are massive.[15] The density distribution is very heterogeneous (Figure 1a), and a small gas clump of size 0.1 pc at a local density peak, which is called a cloud core, has typical masses similar to the Sun or more (see Figure 1b and section 5). Cores are subject to gravitational instability; they are massive enough to collapse due to their own gravity. The cores are supported against collapse by a pressure gradient due to the combination of thermal, magnetic, and turbulent pressure. The cores start collapse to form stars, once the gravity overwhelms the pressure gradient.[16] Detailed structures of cores (Figure 1b,c) are observed to study star-formation processes, e.g., how the mass of a new born star is

Special Issue: 2013 Astrochemistry

Received: June 13, 2013
Published: November 8, 2013

   dx.doi.org/10.1021/cr4003193 | Chem. Rev. 2013, 113, 8961−8980

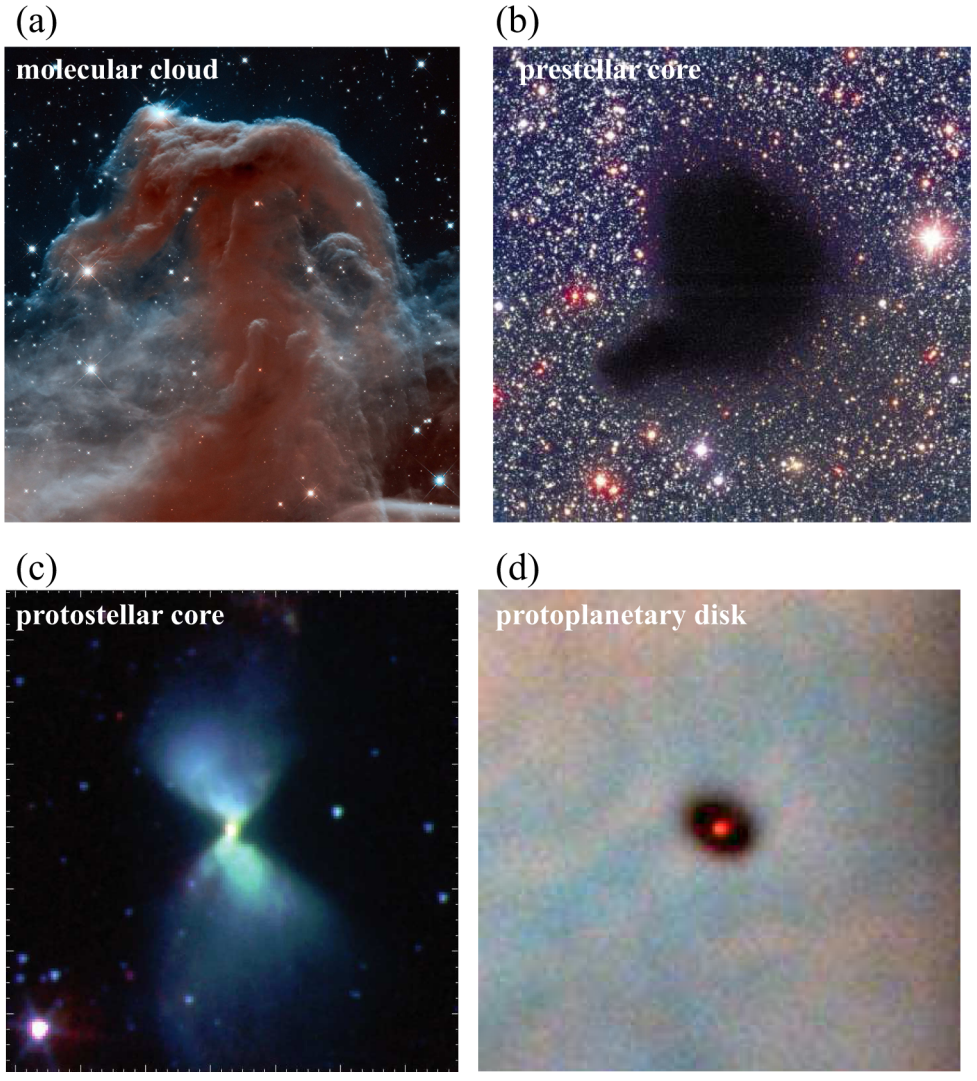

Figure 1. Astronomical objects in the sequence of star formation. (a) Infrared image of Horsehead Nebula, which is a part of Orion Molecular Cloud Complex. The size of the image is about 0.8 pc × 0.9 pc. One pc is about 3.1×10^{16} m, which corresponds to about 2×10^5 times the distance between Earth and Sun. The image is reproduced from NASA, ESA, and the Hubble Heritage Team (AURA/STScI). (b) Barnard 68 (B68), an isolated prestellar core observed in optical and infrared wavelengths using Very Large Telescope. The core looks like a hole on the sky, since the dust grains in the core attenuate the light of background stars. The image size is about 0.26 pc on a side. Reprinted by permission from Macmillan Publishers Ltd.: Nature, ref 7, copyright 2001. (c) Infrared image of a young protostar L1527 IRS (IRAS04368 + 2557) taken by the Spitzer Space telescope. The hourglass shaped blue region is a cavity curved by a bipolar outflow from the central object; the cavity wall reflects the light from the central object. Dense circumstellar material exists in the dark torus region around the central object. The image size is about 28000 AU (0.14 pc) on a side. Reproduced by permission of the American Astronomical Society (AAS) from ref 8, copyright 2008. (d) Protoplanetary disk (dark oval) around a young star (red dot) in Orion Nebula (M42, NGC 1976) observed by Hubble Space Telescope. The image size is about 1.7×10^3 AU (8.5×10^{-3} pc). The image is reproduced from http://www.spacetelescope.org/images/opo9545a/, NASA, ESA, C.R. O'Dell (Rice University), and S. K. Wong (Rice University).

determined and if (and how) multiple stars can be formed in a core. The core before star formation is called a prestellar core, whereas the core harboring protostar(s) are called a protostellar core. Molecular line observations in radio wavelength is a very powerful tool to investigate the core structure,[17,18] since millimeter radiation suffer much less attenuation than shorter wavelength. High spectral resolution of radio telescopes also enable us to investigate dynamics of the core (i.e., the gas velocities) by Doppler shift. The temperature of molecular clouds (~10 K) is, however, too low for molecular hydrogen to emit rovibrational lines. Instead of H_2, heavy-element molecules such as CO are observed. To trace back to H_2, which is the main component of the molecular clouds, we need to know the abundance of molecules relative to H_2. Observations of cloud cores revealed rich chemistry; various molecular lines are detected and their intensities vary among objects.[17−19]

Planets are formed in a disk around a young star, which is called a protoplanetary disk[20] (Figure 1e). The cloud cores have nonzero ($\sim 10^{-14}$ s^{-1})[21] angular momentum. As a core collapses, the rotational velocity increases due to the angular momentum conservation. Eventually, the centrifugal force balances the gravitational force, and a 100 AU-size disk is formed[22,23] (1 AU is the distance between Earth and Sun; $\sim 1.5 \times 10^{11}$ m). The disk should naturally inherit the gas and dust from the parental molecular cloud core; the disk is mainly composed of molecular hydrogen and small dust grains.[24] Heavy-element molecules such as gaseous CO, CN, H_2CO, and H_2O ice are also detected in the disk.[25−27] Within the disk, dust

dx.doi.org/10.1021/cr4003193 | Chem. Rev. 2013, 113, 8961−8980

grains sediment and coagulate to form km-sized rocks, called planetesimals, which then collide with each other and accumulate to form planets. Although planets are mainly made of rocks, volatile elements, such as carbon, oxygen and nitrogen, play a crucial role in determining the surface environments of the planets. Outside the disk radius of ≥ several AU, the disk temperature is so low (≤100 K) that water condenses into ice to be a major building block of planets, together with rocks. Chemistry is thus essential for planetary system formation.

The evolutionary sequence from molecular clouds to planetary systems described above, and the detection of various molecular lines in each evolutionary stage, naturally give rise to many questions. How are the molecules in molecular clouds and cloud cores incorporated to protoplanetary disks? How is the chemical composition altered during the star- and planet-formation processes? What is the major carrier of volatile elements in disks, and how do they vary as a function of time and distance from the central star? Combinations of hydro-chemical models and observation of star-forming cores and disks are powerful tools to tackle these questions. While the chemistry in the disk is reviewed by Henning & Semenov,[28] we will review chemistry in earlier stages, from molecular cloud cores to forming protoplanetary disks. Evolution of water, one of the key molecules for star and planet formation, is reviewed by van Dishoeck et al.[29]

2. BASIC CHEMICAL PROCESSES

It is well established that molecular clouds are, in general, not in chemical equilibrium, because of their low density and low temperature. Molecular abundance and its temporal variation in molecular clouds can be investigated using a chemical reaction network model, a compilation of various possible reactions in molecular clouds.[30−32] These models refer to chemical database such as NIST database, combustion theory,[33] and many laboratory and theoretical work on individual reactions. Accurate evaluation of the rate coefficients and their dependence on temperature, down to ∼10 K, is essential, although such measurements are still limited,[34] compared with the number of reactions included in the network models. In this section, we overview the basic chemical processes in molecular clouds.[35,36]

2.1. Gas-Phase Reactions

First of all, chemical reactions are divided into two categories: gas-phase reactions and grain−surface reactions. The importance of the gas-phase and grain-surface processes vary with physical conditions (see sections 5 and 6). Table 1 summarizes the gas-phase reactions. Among them, cosmic-ray ionization and ion−molecule reactions are the dominant reactions in cold molecular clouds which are well shielded from interstellar UV radiation. Cosmic rays are high-energy (in the range of MeV and GeV) particles mainly composed of protons. The collision of cosmic ray and gas particle produces an ion and a high-energy electron, which further ionizes the gas along the trajectory. The total ionization rate per hydrogen is $\sim 10^{-17}$ s^{-1}.[37]

Table 1. Major Gas-Phase Reactions in Molecular Clouds

reactions		typical value of rate coefficient
cosmic-ray ionization	$A \rightarrow A^+$	10^{-17} s^{-1}
ion−molecule reaction	$A^+ + BC \rightarrow AB^+ + C$	10^{-9} cm^3 s^{-1}
radiative association	$A + B \rightarrow AB + h\nu$	10^{-17}−10^{-9} cm^3 s^{-1}
neutral−neutral reactions	$AB + C \rightarrow A + BC$	10^{-11} cm^3 s^{-1}
radiative recombination	$A^+ + e \rightarrow A + h\nu$	10^{-12} cm^3 s^{-1}
dissociative recombination	$AB^+ + e \rightarrow A + B$	10^{-7} cm^3 s^{-1}

The hydrogen molecule, the dominant composition of clouds, is ionized to be H_2^+, which further reacts with another H_2 to produce H_3^+:[38,39]

$$H_2 + \text{C.R.} \rightarrow H_2^+ + e$$

$$H_2^+ + H_2 \rightarrow H_3^+ + H$$

Due to the low proton affinity of H_2, H_3^+ readily gives its proton to atoms and molecules, e.g.,

$$H_3^+ + O \rightarrow OH^+ + H_2 \quad (1)$$

Subsequent reactions of OH^+ with H_2 and recombination with an electron produce water[40]

$$OH^+ + H_2 \rightarrow H_2O^+ + H \quad (2)$$

$$H_2O^+ + H_2 \rightarrow H_3O^+ \quad (3)$$

$$H_3O^+ + e \rightarrow H_2O + H \quad (4)$$

A similar sequence of reactions makes CH_4. However, a reaction in the sequence

$$CH_3^+ + H_2 \rightarrow CH_4^+ + H \quad (5)$$

is endothermic and forbidden at low temperatures. Further reaction thus proceeds via radiative association[41−43]

$$CH_3^+ + H_2 \rightarrow CH_5^+$$

It should be noted that the radiative association of small molecules is generally slower than ion−molecule reactions (Table 1); the excess energy has to be discarded to stabilize the product (CH_5^+) before it is broken apart. A three-body reaction, which is an alternative way to remove the excess energy, is negligible in molecular clouds due to low density. Methane is finally formed by the dissociative recombination

$$CH_5^+ + e \rightarrow CH_4 + H$$

Ion−molecule reactions of hydrocarbons with carbon ion makes the carbon chains, e.g.,[44]

$$CH_4 + C^+ \rightarrow C_2H_3^+ + H \quad (6)$$

The combination of this reaction and the endothermicity of proton transfer to make saturated molecules such as the reaction 5 explains the fact that various unsaturated carbon chains are detected in molecular clouds. Hydrocarbons and carbon chains are eventually oxidized to form CO, which is the dominant C-bearing species in molecular clouds.

It should be noted that not all ion−molecule reactions proceed efficiently. Unlike O and C, the N atom does not react with H_3^+. The reaction

$$H_3^+ + N \rightarrow NH^+ + H_2 \quad (7)$$

is strongly endothermic, because the proton affinity of N atom is lower than that of H_2. An alternative product channel

$$H_3^+ + N \rightarrow NH_2^+ + H \quad (8)$$

dx.doi.org/10.1021/cr4003193 | Chem. Rev. 2013, 113, 8961−8980

has an activation barrier.[45,46] Then for N atom, neutral−neutral reactions such as those in eqs 9[47,48] and 10[49] are important.

$$N + OH \rightarrow NO + H \quad (9)$$

$$N + NO \rightarrow N_2 + O \quad (10)$$

Neutral−neutral reactions often have activation barriers. Calculation of the potential energy surface and laboratory measurement of the rate at low temperatures are important to evaluate the barrier.[34]

2.2. Grain−Surface Reactions

Dust grains play important roles in chemistry in molecular clouds. The typical size of dust grain is ∼0.1 μm, and the relative number density of grains to hydrogen nuclei n(grain)/n_H is $\sim 10^{-12}$. Note that the density of interstellar gas is often described by a number density of hydrogen nuclei, $n_H = n(H) + 2n(H_2)$, rather than the number density of hydrogen molecule $n(H_2)$, since the ratio of H atom to H_2 varies with physical conditions. At low temperatures, atoms and molecules in the gas phase stick onto grain surfaces on collision to form ice mantle layers. The adsorption time scale of gas phase species onto grains is

$$t_{ads} = \left[S\pi a^2 \sqrt{\frac{8kT}{\pi m}}\, n(\text{grain}) \right]^{-1} \approx 1 \times 10^6 \left(\frac{10^4\ \text{cm}^{-3}}{n_H} \right) \left(\frac{1.0}{S} \right) \left(\frac{0.1\ \mu\text{m}}{a} \right)^2 \text{yr} \quad (11)$$

in which S is the sticking probability, a is the grain radius, and n(grain) is the number density of dust grains ($\sim 10^{-12} n_H$). Theoretical calculations and laboratory experiments show that the sticking probability is high at low temperatures (∼10 K).[50−52]

The adsorbed species migrate over the grain surface and react with each other when they meet. Unlike the gas-phase reactions, association reactions (i.e., two-body reactions to form one product) proceed efficiently by discarding the excess energy onto grain surfaces. As the lightest atom, the H atom could migrate on the grain surface via tunneling. Laboratory experiments, however, show that the migration rate of the H atom depends on the dust temperature; that is, even H atoms migrate via thermal hopping rather than tunneling.[53] Yet the migration of the hydrogen atom is more efficient than that of other atoms and molecules at 10 K. The most important grain−surface reaction would be H_2 formation: $H + H \rightarrow H_2$. Due to its lack of dipole moment, H_2 formation via radiative association ($H + H \rightarrow H_2 + h\nu$) in the gas phase is very inefficient. Once H_2 is formed, various molecules can be formed by ion−molecule reactions in the gas phase (section 2.1).

The hydrogen atom also reacts with other atoms and molecules on grain surfaces. For example, hydrogenation of O atom

$$O + H \rightarrow OH$$

$$OH + H \rightarrow H_2O$$

is more efficient path way to form water than the gas phase reactions of 1−4.[54−56] Indeed, water ice is the dominant component of the ice mantle on interstellar grains in molecular clouds. The abundance of H_2O ice relative to n_H is $\sim 10^{-4}$; about 10% of the elemental abundance of oxygen is tied to water ice.[57] Other saturated molecules, such as CH_4 and NH_3, are also efficiently formed by grain surface reactions.[54,58] Similarly, H_2CO and CH_3OH are formed by hydrogenation of CO, after it becomes abundant in the gas phase and adsorbed onto grains (Figure 2).[59−61]

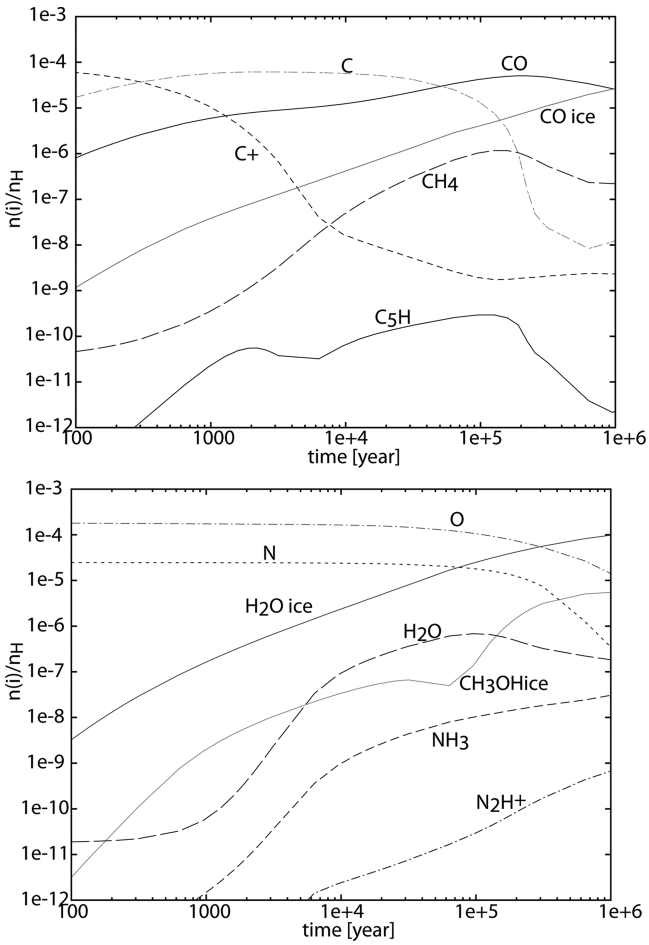

Figure 2. Temporal variation of molecular abundances in a pseudo time-dependent model with T = 10 K and $n_H = 2 \times 10^4$ cm^{-3}. "Ice" means that the molecule is in the ice mantle of dust grains (see section 2).

When the gas and dust temperatures rise due to star formation, hydrogenation becomes inefficient, since the H atom is desorbed to the gas phase before migrating over grain surfaces. Instead, heavy element species can now migrate on grain surfaces to meet a reaction partner, producing complex organic species.[30,62,63]

Adsorbed species and products of grain surface reactions can be desorbed to the gas phase via various mechanisms. First, they can thermally desorb to the gas phase. At the typical temperature of molecular clouds, 10 K, thermal desorption is effective only for H atom, H_2 and He. Various mechanisms of nonthermal desorption are also considered: stochastic heating of dust grains, photodesorption and reactive desorption. Cosmic-rays and X-rays stochastically heat dust grains to desorb atoms and molecules.[64,65] Molecules in ice mantle absorbs UV radiation to be excited or dissociated. A fraction of the kinetic energy of an excited molecule or the products of photodissociation is used to desorb themselves or neighboring molecules.[66−70] When a molecule is formed by a grain−surface reaction, a fraction of the excess energy can be used to desorb the product. For example, theoretical calculation shows that H_2

dx.doi.org/10.1021/cr4003193 | Chem. Rev. 2013, 113, 8961−8980

can efficiently desorb to the gas phase upon formation.[71,72] The excess energy could also be used to desorb the neighboring molecules in the ice mantle.[73]

3. PSEUDOTIME DEPENDENT MODEL

Using the set of reactions described above, we can write the rate equation

$$\frac{dn_i}{dt} = \sum_j \alpha_j n_j + \sum_{j,k} \beta_{jk} n_j n_k \quad (12)$$

where n_i is the number density of species i and α and β are reaction rate coefficients. The first term on the right-hand side represents the reactions with external particles; for example, species i is formed by photodissociation of species j or species i (= j) is destroyed by cosmic-ray ionization. The second term represents two-body reactions in which species i is formed by the reaction of species j and k or species i (= j) is destroyed by the reaction with species k. For the destruction terms, α and β becomes negative in eq 12. The rate coefficients, (the absolute value of) α and β, depend on physical parameters such as cosmic ray ionization rate, UV flux, and temperature of gas and dust. We write down the rate equations for all relevant species, and solve them simultaneously. It should be noted that the rate equations are nonlinear equation of gas density; the solution of the equations depends on the density.

Equation 12 is an initial value problem; given the initial molecular abundances, the temporal variation of the abundances is calculated. It is usually assumed that gaseous species are in atomic form or ionized at $t = 0$, depending on whether the ionization potential of the atom is higher than 13.6 eV; that is, carbon is ionized, but nitrogen and oxygen are in atomic form.[74] Hydrogen is assumed to be in molecular form, H_2, initially, since a significant amount of hydrogen is considered to be in H_2 even in diffuse clouds, which are interstellar clouds with much lower density ($n_H \approx 10^2$ cm^{-3}) than molecular clouds, and since molecules cannot be formed efficiently without H_2 (section 2). Considering the dominant abundance of hydrogen in the interstellar gas and the self-shielding effect,[75,76] H_2 should be the first to be formed in molecular clouds.[77]

Figure 2 shows the temporal variation of assorted molecular abundances obtained by a chemical reaction network model at a typical molecular cloud condition (T = 10 K and $n_H = 2 \times 10^4$ cm^{-3}). The vertical axis is the abundances relative to hydrogen nuclei n_H. The upper panel of Figure 2 depict evolution of carbon; carbon ion, which is set abundant initially, is first converted to carbon atom, and then to CO. At the latest moment ($t \approx 10^6$ yr), CO is converted to CO ice. Oxygen, on the other hand, is in atomic form initially and converted slowly to H_2O ice. We can see that carbon chains (e.g., C_5H) are abundant at $\sim 10^5$ yr, while NH_3 and N_2H^+ become abundant at $\geq 10^6$ yr.

How does the chemical reaction network model compare with the observations of molecular clouds? It is interesting that radio observations find line emissions of carbon chains to be weak in cloud cores which are bright in NH_3 lines, and vice visa.[78,79] In comparison with the theoretical models (Figure 2), cloud cores with high abundances of NH_3 are considered to be "chemically old", while the cores with carbon chains are "chemically young". It should be noted that the model shown in Figure 2 is a very simplified one; it calculates temporal variation of molecular abundances, while the physical conditions (density and temperature) are fixed; it is called pseudotime dependent model. In reality, molecular clouds are considered to be formed by accumulation of less dense gas, during which gas density, temperature, and attenuation of interstellar radiation should vary.[80−82] Observations show that gas density is never uniform in molecular clouds; recent observations by Herschel Space Observatory revealed that molecular clouds are made of filaments with density fluctuations.[83−85] The coincidence of temporal variation of molecular abundances in the model with spatial variation of molecular abundances (i.e., spatial segregation of carbon chains and NH_3) indicates, however, that the pseudotime dependent model correctly depicts the molecular evolution in molecular clouds, at least qualitatively. At t = several 10^5 yr, the pseudotime dependent models[86−88] actually well reproduce abundances of many molecules detected in a cloud core Taurus Molecular Cloud 1 (TMC1). Since TMC1 shows many molecular lines but no sign of star formation, it has been a target of intensive molecular line surveys[9,89,90] to understand the cold chemistry without the perturbation of star formation.

4. CHEMISTRY IN THE FLOW

Although the molecular abundances calculated by the pseudotime dependent model show reasonable agreements with observation, it is important to couple the rate equations with hydrodynamics to understand the physical and chemical evolution of interstellar clouds, considering their dynamical nature. In astrophysics, the aim of the combined calculation of the hydrodynamics and chemical rate equations are 3-fold. First, atoms and molecules in interstellar gas work as coolants via emission of photons. In order to determine the temperature of the gas, which in turn determines the pressure and thus affects the dynamics, abundances of chemical species should be calculated. Star formation in the early universe is a good example. A star is formed by a gravitational collapse of gas. If there is no coolant, i.e., if the gas is adiabatic, the gas is heated by compression and the collapse is halted by the increasing gas pressure. In the current universe, gravitational energy released by the collapse is efficiently radiated away by thermal emission of dust grains. However, in the early universe, elements heavier than helium are practically absent. The cooling rate of the gas, and thus the star formation process, critically depends on the abundance of H_2 and HD, which are the major coolant in the absence of heavy elements.[91−94] Another example is interstellar shock waves. Supersonic flows are ubiquitous in interstellar space,[95] e.g., supernovae, stellar winds from evolved stars, and bipolar outflow from young stellar objects (YSOs). Transition of the supersonic flow to subsonic flow is accompanied by a shock wave, in which the gas is compressed and the kinetic energy of the bulk motion is converted to the thermal energy of gas.[96] If the gas is adiabatic, the sharp rise of gas temperature enhances the pressure so that the density enhancement becomes rather small, e.g. $\leq$4 in atomic gas, even in a very strong shock. If the gas is cooled by emission of lines, the post shock gas can be much denser than the adiabatic case. Since the atomic and molecular lines (i.e., C^+, O atom, and CO) are more efficient as a coolant than dust grains in the density range of interstellar shocks,[97,98] the combined calculation of hydrodynamics with chemistry is important. The combined calculation is, however, computationally demanding, especially in the case of multidimensional (2D or 3D) hydrodynamic simulations. These studies usually include a relatively small

dx.doi.org/10.1021/cr4003193 | Chem. Rev. 2013, 113, 8961−8980

chemical network, with the number of chemical species restricted to less than a few tens.[82,98−101]

Second, molecular abundances are used as tracers of the physical structure and/or evolutionary stage of hydrodynamic systems in comparison with observations. Figure 2 shows that molecular abundances in clouds change over 10^5−10^6 yr. On the other hand, the free-fall time scale of isothermal gas, in which the radiative cooling is efficient enough to keep the gas temperature cool, is

$$t_{\rm ff} = \sqrt{\frac{3\pi}{32\rho G}} \approx 4 \times 10^5 \left(\frac{10^4\ {\rm cm}^{-3}}{n_{\rm H}}\right)^{1/2}\ {\rm yr} \tag{13}$$

where G is the gravitational constant and ρ is the mass density of the gas.[102] The similarity of the chemical and dynamical time scale indicates that the molecular abundances would change during the contraction, producing the radial gradient of molecular abundances. Eventually the central part of the core becomes optically thick to thermal radiation. Then photons cannot freely escape from the system, and the core temperature rises, which further affect the chemistry. In the last decades, radio observations revealed that molecular abundances vary within cores, as well as among cores.[17,103,104] Molecular distribution and its temporal variation can be investigated by solving the rate equations in multiple Lagrangian fluid parcels (see below).

Third, the similarity of the chemical and dynamical time scale also indicates that we have to consider hydrodynamic evolution of gas to understand the chemical evolution. When the gas density rises (declines), the collision among gas phase species becomes more (less) frequent, and the reaction becomes faster (slower). However, the chemical time scale as a whole is not simply proportional to the inverse of density and should be investigated numerically, because the rate equation is nonlinear (eq 12). Temporal variation of the temperature significantly affects the rates of desorption and grain-surface reactions. For example, complex organic molecules can be formed by grain surface reactions in warm regions around young stars[30,62,63] (sections 2 and 6). Since the gas around a young star is falling toward the central star, the duration of such warm phase and thus the amount of complex organic molecules formed on grain surfaces depend on the size of the warm region divided by the infall velocity.

The basic equation of hydrodynamics consists of three conservation equations: conservation of mass, momentum and energy. For example, the conservation of mass is expressed as

$$\frac{\partial n_i}{\partial t} + \nabla\cdot(n_i\vec{v}) = S \tag{14}$$

where n_i is number density of species i at a position we are interested in. The velocity $\vec{v}$ is determined by the conservation of momentum (i.e., equation of motion). The source term S is zero, if there is no formation or destruction of species i; the temporal variation of number density at the position is simply determined by the spatial divergence of flux $(n_i\vec{v})$. In the case of flow with chemical reactions, S is the sum of formation rate (positive value) and destruction rate (negative value), i.e., the right-hand side of eq 12.

Equation 14 gives the temporal variation of number density n_i at a specific position; it is called Eulerian specification of the flow field. In the calculation of molecular evolution with hydrodynamic flow, Lagrangian specification is more convenient; it describes the temporal variation of n_i and other parameters such as $\vec{v}$ along the flow. In other words, we follow moving fluid parcels. The Lagrangian derivative is given as

$$\frac{{\rm D}n_i}{{\rm D}t} = \frac{\partial n_i}{\partial t} + (\vec{v}\cdot\nabla)n_i \tag{15}$$

By applying the chain rule to eq 14 and by replacing $\partial/\partial t$ by ${\rm D}/{\rm D}t$, we can obtain

$$\frac{{\rm D}n_i}{{\rm D}t} + n_i(\nabla\cdot\vec{v}) = S \tag{16}$$

If we rewrite the number density of species n_i as $n_{\rm H}x$ by defining x as abundance $n_i/n_{\rm H}$, the above equation becomes

$$\frac{{\rm D}(n_{\rm H}x)}{{\rm D}t} + (n_{\rm H}x)(\nabla\cdot\vec{v}) = S \tag{17}$$

Since the total number of hydrogen nuclei is conserved

$$\frac{{\rm D}n_{\rm H}}{{\rm D}t} + (n_{\rm H})(\nabla\cdot\vec{v}) = 0 \tag{18}$$

the temporal variation of the abundance along the flow is described as

$$n_{\rm H}\frac{{\rm D}x}{{\rm D}t} = S \tag{19}$$

Note that it does not have the advection term; it means that the molecular abundance is determined by the reactions within a fluid parcel. It makes the calculation simple; we can calculate a set of rate equations in each fluid parcel in the flow separately, rather than considering all fluid parcels at once.

In sections 5 and 6, we will review chemical models of star-forming cores paying special attention to the interplay between dynamical and chemical evolution.

5. PRESTELLAR CORES

Prestellar cores are dense and cold gas clumps which are bounded by the self-gravity. Figure 3 shows a well-known prestellar core B68 observed with various wavelength. It is 125 pc away from the Earth.[105] The core is about twice as massive as the Sun, and its size (outer radius) is ∼10^4 AU.[7] The thermal radiation of dust grains at submillimeter (Figure 3b) has the peak at the core center; since the small grains are well-mixed with gas, the gas density must be also centrally peaked. There are several other well-investigated prestellar cores, such as L1544 and L1498.[17,18] The typical number density of H_2 at the center of prestellar cores ranges from 10^5 cm^{-3} to 10^7 cm^{-3}, and the temperature is ∼10 K or below.

The density distribution inside the prestellar core is similar to the Bonnor−Ebert spheres, which are the isothermal equilibrium (gravity balances with pressure gradient) spheres with various central densities.[7,106,107] While the infalling motion is observed toward some cores via Doppler shift of the molecular lines, some cores do not show infall signatures and thus are considered to be in equilibrium state.[107−109] In these dense cores without infall motions, the molecular line width is dominated by thermal broadening; the ratio of turbulent and thermal pressure is less than 40%.[110] Magnetic field could also contribute to support the core,[111] although the observations show that the magnetic fields in could cores are not strong enough to dominate over the gravity.[112] Keto and Caselli[113] investigated the stability of cold gas sphere with detailed analysis of the thermal structure (temperature distribution) , and showed that the gas sphere becomes gravitationally

dx.doi.org/10.1021/cr4003193 | Chem. Rev. 2013, 113, 8961−8980

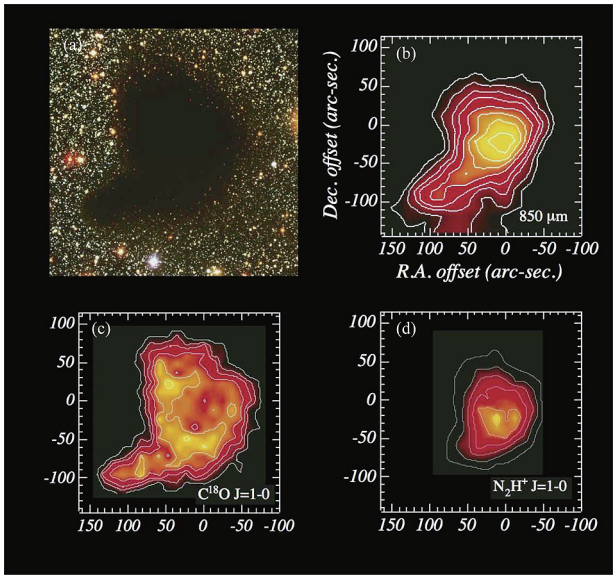

Figure 3. Observation of Barnard 68 in various wavelengths summarized in ref 17. (a) Optical image, (b) 850 μm dust continuum emission, (c) $C^{18}O$ emission line, and (d) N_2H^+ emission line. The size of the image is about 0.15 pc × 0.15 pc. Republished with permission from ref 17. Copyright 2007 Annual Reviews; permission conveyed through Copyright Clearance Center, Inc.

unstable if the central density exceeds $\sim 10^5$ cm^{-3} and that this critical density depends on other parameters such as the total mass.

Once the gravity overwhelms the pressure, the core collapses. Figure 4a,b shows the radial distribution of density and infalling velocity in a model of collapsing core. At t = 0, the central density is $\sim 10^4$ cm^{-3}, and the total mass of the core is ~4 solar mass; the self-gravity slightly overwhelms the thermal pressure. Then, the central density increases as the contraction proceeds, e.g., it reaches $n_H = 3 \times 10^6$ cm^{-3} at $t = 1.15 \times 10^6$ yr. We also note that the contraction accelerates (i.e., the contraction time scale decreases) as the central density rises, which is expected from eq 13. Figure 4c–f show the radial distribution of molecules in the gas phase (c and e) and in ice mantle layer (d and f) in the collapsing core when the central density of the core is $n_H = 3 \times 10^6$ cm^{-3}. It is obtained by calculating the rate equations in many fluid parcels which reach different radii at the time step we are interested in.

5.1. Molecular Depletion and Chemical Fractionation

Due to the low temperature and high density, heavy-element species are frozen onto grains in the central region of the prestellar cores. It should be noted here that the adsorption time scale (eq 11) is similar to the free-fall time scale of a core at the typical density of molecular clouds $\sim 10^4$ cm^{-3} (eq 13). The adsorption time scale is proportional to n_H^{-1}, while the free-fall time scale is proportional to $n_H^{-1/2}$; that is, the adsorption time scale becomes shorter than the free-fall time scale at higher densities. It naturally explains molecular depletion observed in prestellar cores.[103,115,116]

Figure 3c shows the intensity of $C^{18}O$ line in B68. We can see that the CO emission is bright in outer radius but weak in the central region of the core, which indicates that CO is depleted at the core center (Figure 4c). Such a CO "hole" is observed toward several prestellar cores.[17,18] We can derive the depletion factor, the ratio of the canonical abundance in molecular clouds (e.g, $n(CO)/n_H = 10^{-4}$) to the estimated molecular abundance at the core center by comparing the molecular line map (Figure 3c) with the dust continuum map (Figure 3b). The CO depletion factor varies among objects and range from a few to 10^2.[109,116] It should be noted that such molecular depletion becomes apparent thanks to the high-spatial resolution observations of dust continuum and molecular lines at submillimeter and millimeter. Before these observations become available, there was not convincing evidence of significant (order of magnitude) depletion of molecules in the gas phase, although it had been known from the infrared observation of ice absorption bands that some fractions of H_2O and CO are frozen onto grains.[57]

Although neutral heavy-element molecules are, in general, subject to depletion onto grains, the depletion factor is found to vary among molecules[103]. It is called chemical fractionation. While the depletion factor of CO (and other C-bearing species) reach ≥100 at the center of very dense prestellar cores, N-bearing species are more resilient against depletion. For example, we can see in Figure 3d that N_2H^+ emission is bright inside the hole of CO emission. Models and observations[117−119] indicate that nitrogen molecules are slow to form in molecular clouds (section 2). Formation of N-bearing molecules from N atom, which is more volatile than CO, temporarily compensate the depletion. In Figure 4c we can see that depletion region of NH_3 and N_2H^+ are indeed smaller than that of CO.

Since CO is the most abundant molecule made of elements heavier than He, the CO depletion has significant impacts on the chemical reaction network. For example, CO is the dominant reactant of N_2H^+. CO depletion thus temporarily helps to keep N_2H^+ abundant in the gas phase at the core center.[117,120]

Equation 11 indicates that the adsorption time scale is inversely proportional to the total surface area of grains, $\pi a^2 n$(grain). In the right-hand side of eq 11, we assumed that the dust grains have a uniform radius of 0.1 μm. In reality, grains have a size distribution, which is modeled by many groups such as Mathis et al.[121] and Weingartner and Draine.[122] The total surface becomes larger or smaller than the uniform 0.1 μm dust case by a factor of 2−3 depending on the grain models, and the adsorption time scale changes accordingly.[123] Acharyya et al.[123] calculated gas-grain chemistry considering the grain size distribution; they found that the models with a uniform grain size can be a reasonable approximation for chemistry, as long as the dust temperatures do not depend on the grain size. Flower et al.[124] investigated chemistry in collapsing prestellar core considering coagulation of dust grains. They showed that the mean grain radius increases at most by a factor of ~5 by the time the central density of the core reaches 10^6 cm^{-3}. They also found that the effect of grain growth on the freeze-out of neutral molecules are modest, while the major ion molecule changes depending on the grain size, since recombination of atomic ion (such as H^+) is more efficient on dust grains than in the gas phase (with free electron).

5.2. Deuteration

Another important outcome of CO depletion is the enhancement of deuterium fractionation. In molecular clouds with $T \leq$ several 10 K, the D/H ratio of molecules, XH/XD, are higher than the elemental abundance of D/H = 1.5×10^{-5} [125]. For example, the DNC/HNC ratio ranges from 0.02 to 0.09 in nearby molecular cloud cores.[126] It is well established that the

dx.doi.org/10.1021/cr4003193 | Chem. Rev. 2013, 113, 8961−8980

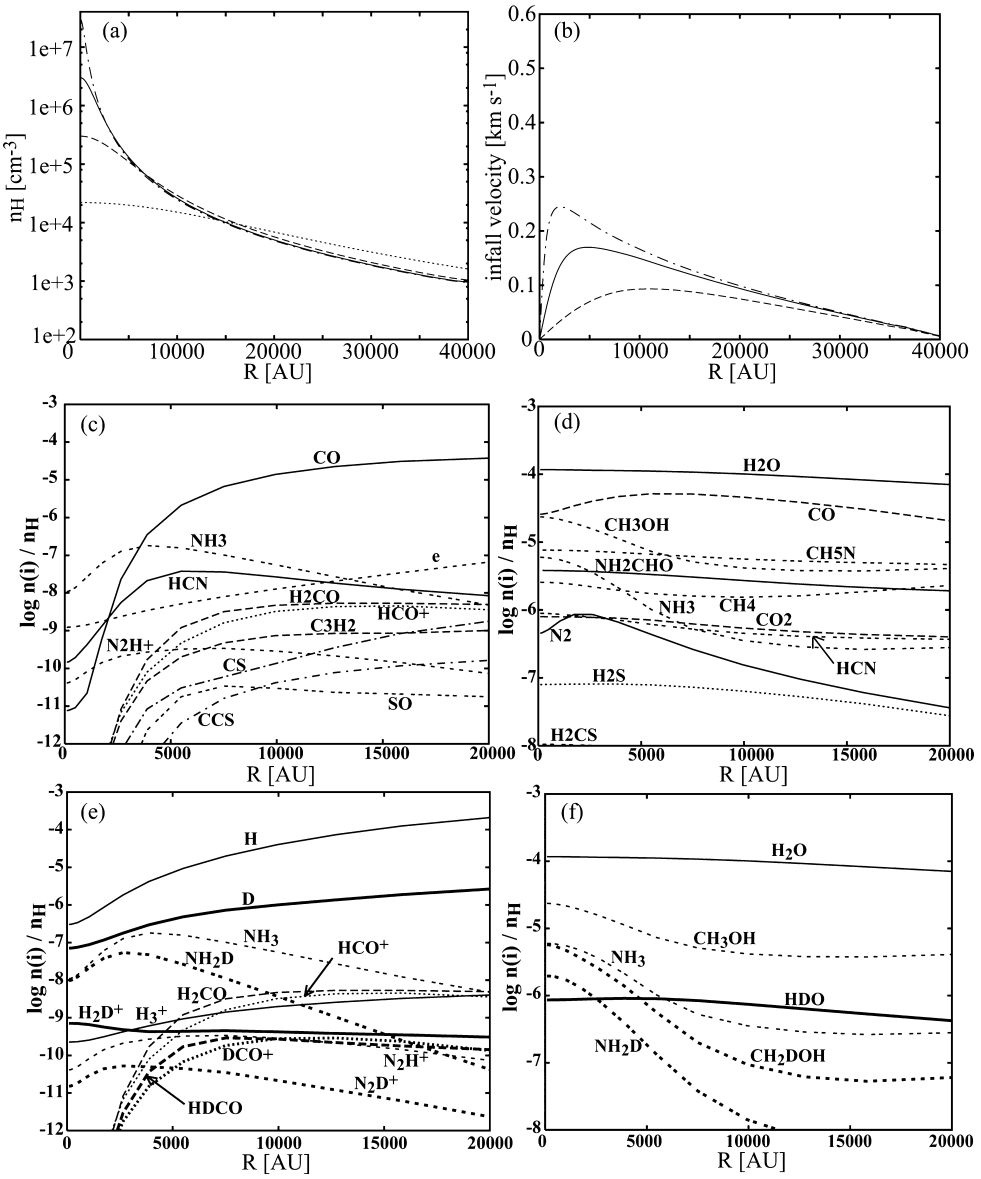

Figure 4. Radial distribution of (a) density and (b) infall velocity in a model of collapsing prestellar core at t = 0 (dotted line), 1.05 (dashed line), 1.15 (solid line), and 1.17 Myr (dot-dashed line). The infall velocity is zero at t = 0. Distribution of molecular abundances at 1.15 Myr are shown in panels c–f; panels c and e present the gas-phase abundances, while panels d and f present the ice abundances. Figure adapted from ref 114 by permission of the AAS, copyright 2005.

enhancement is due to exothermic exchange reactions.[127,128] The most important exchange reaction is

$$H_3^+ + HD \rightarrow H_2D^+ + H_2 \quad (20)$$

which is exothermic by 230 K.[129] Since the backward reaction is practically inhibited at 10 K, H_2D^+/H_3^+ ratio is enhanced. Multiply deuterated H_3^+ are formed by similar reactions.[128] Since H_3^+ is the key reactant in the ion–molecule reactions (section 2), the high D/H ratio of H_3^+ propagates to heavy-element molecules.

Deuterated H_3^+ is destroyed by the reactions with CO and electron

$$H_2D^+ + CO \rightarrow HCO^+ + HD \text{ or } DCO^+ + H_2 \quad (21)$$

$$H_2D^+ + e \rightarrow HD + H \text{ or } H_2 + D \quad (22)$$

The recombination of deuterated H_2D^+ (reaction 22) (and its multideuterated analogues) enhance the abundance of D atom, which then participates in the hydrogenation reactions on grain surfaces to make deuterated ice. Considering the balance between formation (20) and destruction (21 and 22), the D/H ratio of H_3^+ is calculated to be

$$\frac{n(H_2D^+)}{n(H_3^+)} = \frac{k_{20}n(HD)}{k_{21}n(CO) + k_{22}n(e)}$$

It shows that decline of CO abundance further enhances the H_2D^+/H_3^+ ratio, and thus deuterium fractionation in other molecules. This theory is supported by the observations of positive correlation of CO depletion factor with deuterium enhancement, and high abundances of H_2D^+ and D_2H^+ in CO depleted cores.[116,130,131]

It should be noted that the deuterium fractionation also depends on the ortho–para ratio of H_2. The lowest state of

dx.doi.org/10.1021/cr4003193 | Chem. Rev. 2013, 113, 8961–8980

ortho-H_2 lies approximately 170 K above the ground state of para-H_2. This internal energy of ortho-H_2 helps overcome the endothermicity of the backward reaction of 20. Flower et al.[132] investigated the D/H ratio of H_3^+ in prestellar cores by distinguishing the nuclear spin states of H_2, H_2^+, and H_3^+ and its deuterated isotopologues. They assumed that the gas density increases with time via free-fall (eq 13) and found that the dynamical effect is important; the o/p ratio and thus the D/H ratio at each collapse stage (i.e., gas density) deviate from the steady state values of pseudotime dependent model at the same density, since the dynamical time scale is much shorter than some of the chemical time scales. In order to reproduce the observed abundances of ortho-H_2D^+ and para-D_2H^+ in prestellar cores, the initial ortho-para ratio of H_2 should be $\leq 3 \times 10^{-2}$ (see Figure 6 in Flower et al.[132]).

5.3. Variation among Cores

Observations show that the CO depletion factor and molecular D/H ratio vary among objects. Since the adsorption is more efficient in higher density cores (eq 11), it is straightforward to use these values as a probe of core evolution; that is, cores with higher depletion factor and molecular D/H ratios should have higher central densities and are more evolved. Indeed, Doppler shift observations of molecular lines show that objects with higher depletion factors are more likely to be infalling toward the core center.[109]

It is also found, however, that the depletion factor varies among objects with similar central densities.[104,133,134] It tells us that these cores have different physical structures and/or histories. For example, Keto and Caselli[113] showed that the cores with $\sim 10^5$ cm^{-3} could be stable or unstable depending on the parameters such as the total mass. Even if the cores are collapsing, the collapse time scale should vary among cores depending on the initial pressure to gravity ratio. If the core is initially close to the equilibrium, for example, the collapse time scale becomes longer than the free-fall time scale given by eq 13. Since CO depletion proceeds with time, the depletion factor would be larger in cores with longer contraction time scale or have been in equilibrium state for a longer time. In other words, the CO depletion would be less significant in cores with shorter collapse time scale.[114,117,135,136] One caution for such interpretation is that it is observationally not clear if the cores with smaller CO depletion factor are really collapsing faster. Although these cores show larger line width (i.e., larger infall velocity or velocity dispersion) than other cores, the difference is only a factor of ~ 2,[133,137] which might not be enough to account for difference in CO depletion. Variety of molecular abundances among cores could also originate in other parameters such as cosmic-ray ionization rate, elemental abundances, magnetic fields, and core temperature.[138,139]

6. PROTOSTELLAR CORES

As the cloud core collapses, compressional heating eventually overwhelms the radiative cooling in the central region (Figure 6). The temperature rises, and the collapse pauses temporarily to form a hydrostatic core made of molecular hydrogen, which is called the "first core". The central density and temperature continue to rise as the gas around the first core falls onto it. When the central temperature reaches ~ 2000 K, hydrogen molecules dissociate. Since the dissociation is endothermic, it practically reduces the pressure so that the core collapses again. The protostar is born when the dissociation completes and the central region of the core reaches the hydrostatic equilibrium again.[140] The new-borm protostar is embedded in a dense gas of parental cloud core, which is called protostellar envelope. The envelope gas will eventually accrete onto the protostar or be expelled from the system by the bipolar outflow from the central region (Figure 1c, 6, and 8). The protostellar core is defined as a molecular cloud core which contains protostar(s). In other words, a protostellar core consist of protostar(s) and envelope gas.

6.1. Hot Cores

Chemistry in protostellar core is characterized by the warm temperature; the envelope gas is heated by the protostar. The shock wave caused by a collision of the bipolar outflow with envelope gas could also heat the gas. Molecules frozen onto grains in the cold prestellar phase are desorbed to the gas phase and restart the gas phase reactions. Endothermic reactions can proceed depending on the endothermicity and the gas temperature of the region.

Such warm gas has long been observed in high-mass star forming region, where stars more massive than Sun are formed, and are called hot molecular cores.[141] Typical density and temperature of hot cores are $n_H \approx 10^6$–10^7 cm^{-3} and $T = 200$ K, respectively.[142] Observations found that saturated molecules, such as NH_3 and CH_3OH, and complex organic molecules (COMs), such as $HCOOCH_3$ are more abundant in hot cores by orders of magnitude than cold molecular clouds.[143−145] The high abundance of saturated molecules, which are formed more efficiently by grain-surface reactions than gas-phase reactions (section 2), and their high D/H ratio[146] indicates that these molecules are not formed in situ but formed in the cold prestellar phase and sublimated in the hot cores.

Brown et al.[147] constructed a model of hot core chemistry; they calculated time-dependent chemistry in which density and temperature changes by three steps. In the first stage, the gas is cold (10 K) and the density increases with time via the free-fall collapse (eq 13). In the second stage, the temperature rises in a short time scale and ices are sublimated. Chemistry in the warm gas (200 K) with sublimates are calculated in the third stage. Brown et al.[147] showed that the abundant saturated molecules such as NH_3 in the hot core indeed originate in the cold stage. Charnley et al.[148] investigated the chemistry in the third stage in more detail. Instead of solving the chemistry in the cold phase, the initial ice abundances (which is immediately sublimated at the start of the model) are given as a free parameter, which is constrained by the observed hot core versus cold cloud abundances, observations of interstellar ice, and previous theoretical models. Charnley et al.[148] found that and CH_3OCH_3 and $HCOOCH_3$ are formed by the gas-phase reactions starting from sublimated CH_3OH and H_2CO; that is, CH_3OH is protonated ($CH_3OH_2^+$) and undergo ion−molecule reactions with other species to form large ion molecules, which eventually recombine to form neutral COMs.

Charnley et al.[148] also showed that the variation of molecular abundances among the warm gases in high-mass star-forming regions[145] are explained by the initial abundance of NH_3 ice and CH_3OH ice; if NH_3 ice is abundant, N-bearing organic species become abundant, while O-bearing species become abundant if the initial ice abundance of CH_3OH is high. The core temperature (i.e., 100 K vs 300 K) is another factor to account for the variation.[149] Charnley[150] showed that SO and SO_2 could be a chemical clock in the hot core, since the sublimated H_2S is converted to SO and then SO_2 in a few 10^4 yr.

dx.doi.org/10.1021/cr4003193 | Chem. Rev. 2013, 113, 8961−8980

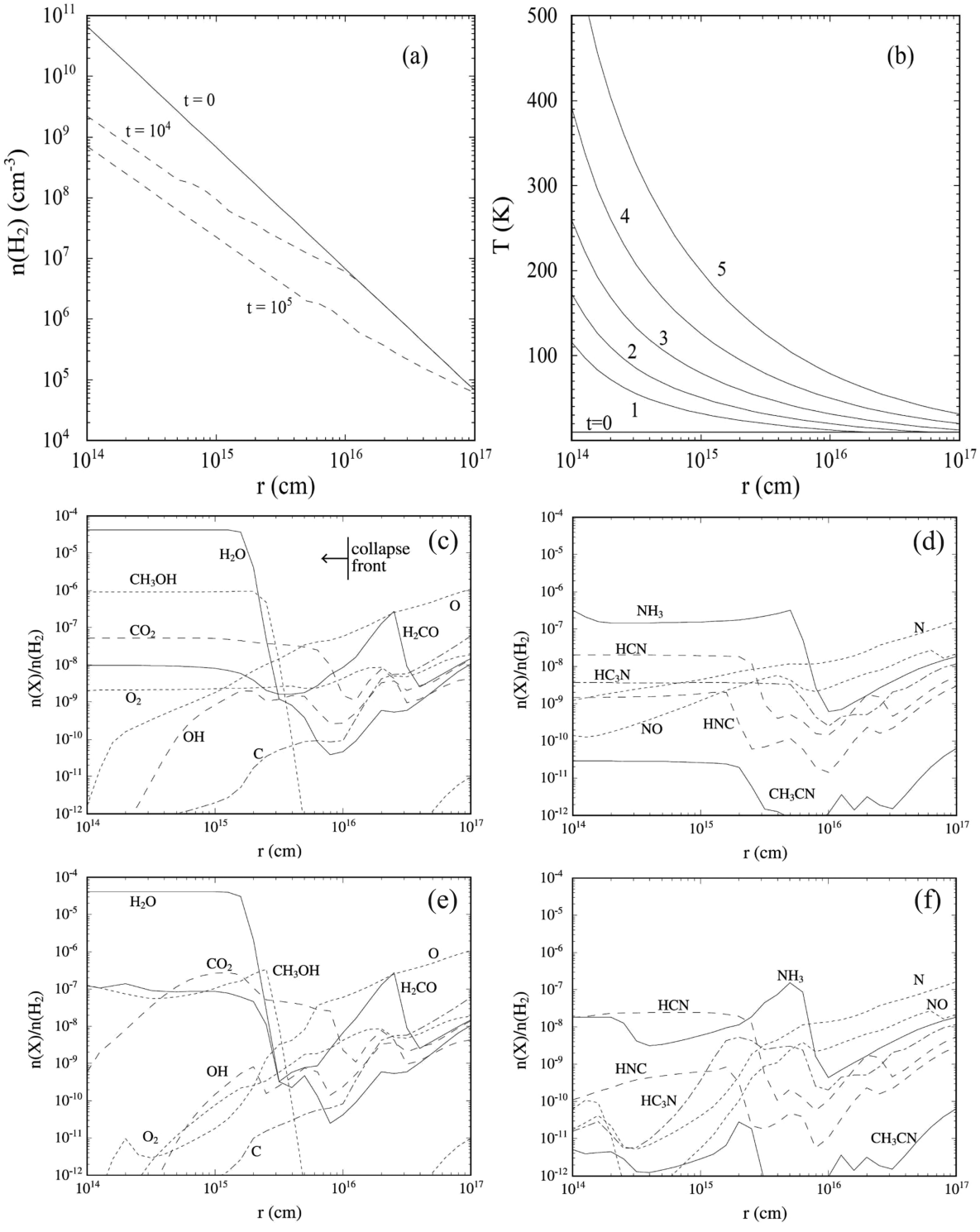

Figure 5. Radial distribution of physical parameters (a-b) and molecular abundances (c–f) in a protostellar core model in ref 156. (c and d) Distribution of molecules in a collapsing core at 10^4 yr. (e and f) Molecular abundances in the core with the same density and temperature distributions but without collapse (i.e., the core is static). Figure adapted from ref 156 by permission of the AAS, copyright 2003.

While the models mentioned above calculate chemistry in one gas clump (i.e., a single point), Doty et al.[151] and Nomura and Millar[152] calculate spatial distribution of molecules in a hot core. They consider radial distribution of density and temperature in the core and calculate the pseudotime dependent model at each radial point (i.e., at given density and temperature). In the model of Doty et al.,[151] the distribution of gas density and temperature are determined based on the observation of a high-mass hot core AFGL2591,[153,154] while Nomura and Millar[152] determined temperature distribution by solving the radiation transfer in a core. The initial molecular abundance is determined referring to the ice observation and previous hot core models.[148] Although Doty et al. and Nomura and Millar compare their models with different objects, AFGL 2591 and G34.3 + 0.15,

dx.doi.org/10.1021/cr4003193 | Chem. Rev. 2013, 113, 8961–8980

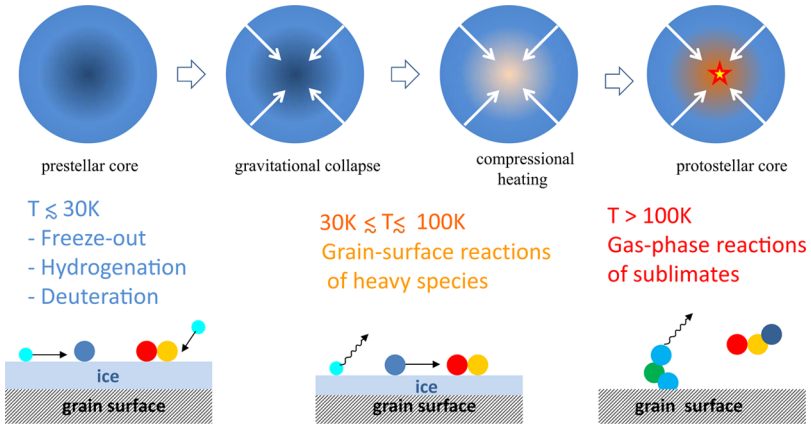

Figure 6. Schematic view of the core evolution and chemical processes in the infalling fluid parcel.

respectively, they both find the best agreement between the model and the observation around 10^4 yr.

Ceccarelli et al.[155] and Rodgers and Charnley[156] went one step further; they calculate the radial distribution of molecules and its temporal variation in a collapsing protostellar core. They adopt the well-known inside-out collapse model by Shu et al.[157] and temperature distribution model by Adams and Shu.[158] The inside-out collapse starts with a static ($v = 0$) isothermal sphere, in which the gas density increases inward as $n \propto r^{-2}$. The free-fall starts from the core center, and the collapse region expands outward with the sound speed. The chemistry is solved in infalling shells, in which the temperature and density increases with time. Figure 5 shows spatial distribution of physical parameters and molecular abundances at 10^4 yr; the molecular distribution shows an onionskin type structure, with more volatile molecules being released at larger distances. To investigate the effect of the dynamics on chemistry, Rodgers and Charnley[156] also calculated molecular abundances in a static core with the same temperature distribution as the dynamical model (Figure 5e,f). In the dynamical model, the radial variation of the molecular abundances are less significant than the static model, because the free-fall time scale is shorter than the chemical time scale in the central region.

6.2. Low-Mass Protostellar Cores

While the hot saturated molecules in high-mass star forming regions have been observed since 1978,[143] intensive molecular line observations toward low-mass protostellar cores started in more recent years,[116,159−172] since the low-mass protostars are much fainter and thus need higher sensitivity than high-mass protostars. The molecular line profiles both in the radio and infrared wavelengths indicate the infall motion of the envelope gas.[173,174]

In the central warm regions of the low-mass protostellar core, two specific chemical phenomena are found: hot corinos and warm carbon chain chemistries. Hot corinos are low-mass protostellar cores with COMs in the central region;[116] i.e. it is the low-mass version of the hot core. For example, HCOOH, $HCOOCH_3$ and CH_3OCH_3 are detected toward IRAS 16293.[163,165,166,177] $HCOOCH_3$ is also detected toward NGC1333 IRAS 4A and 4B.[178−180] To mimic the chemistry in protostellar cores, Garrod and Herbst[62] performed gas-grain chemical network calculations, in which temperature rises with time following a simple power law $T(t)-T(t = 0) \propto t^2$, in time scales of 5×10^4, 2×10^5, and 1×10^6 yr. They found that the grain-surface chemistry during the warm-up phase is important for the formation of COMs. As described in section 2, the association reactions, e.g., CO + H → HCO and HCO + CH_3O → $HCOOCH_3$, are much more efficient on grain surfaces than in the gas phase. Garrod and Herbst[62] show that the formation of COMs on warm grain surfaces is more important in the models with longer warm-up time scales. As in previous hot core models, the grain-surface hydrogenation of CO at low temperature (∼ 10 K) to form H_2CO and CH_3OH and the gas-phase reactions of sublimates in the warm gas also contribute the formation of COMs. However, the efficiency of gas-phase formation of COMs depends on the products and branching ratios of the dissociative recombination of the ion molecules such as $CH_3OCH_4^+$; if the recombination mainly produces, for example, CH_3 + CH_4 + O, rather than CH_3OCH_3 + H, the production of COMs in the gas phase is less efficient than otherwise. In the past decade, laboratory experiments have shown that in the recombination of large ion molecule XYH^+, the main product would be X + YH, rather than XY + H.[181] In other words, the branching ratio is unfavorable for the gas-phase formation of COMs, although the gas-phase path can still be effective for some species.

Sakai et al.[168,182] detected various carbon chains in the protostellar core L1527 (Figure 1d) and IRAS 15398-3359. Since the carbon chain abundances have a peak in the central warm region and since the carbon chains are generally deficient in star-forming cores, they suggested that the detected carbon chains are formed in the gas phase from sublimated CH_4, rather than a remnant of the "chemically young" cloud gas. This mechanism of carbon chain reformation, named as warm carbon chain chemistry (WCCC), is confirmed by the reaction network model by Hassel et al.[81,183] and Aikawa et al.[184] Sakai et al.[185] also found that carbon chains are deficient in hot corinos, while COMs are deficient in WCCC cores. Such differences in chemical composition may originate in the collapse time scale of prestellar cores. If the collapse time scale is longer than that of CO formation in the gas phase, CO ice would become abundant, which then converted to CH_3OH and COMs. If the core collapses faster, on the other hand, CH_4 ice becomes abundant, and WCCC will eventually take place.[186]

6.3. Chemistry in Radiation-Hydrodynamic Models

Although the basic formation paths of COMs and carbon chains are understood as described above, a combination of these gas-grain chemical models with realistic hydrodynamic models is useful to answer further questions such as (a) how do the abundances of COMs and carbon chains vary along the

dx.doi.org/10.1021/cr4003193 | Chem. Rev. 2013, 113, 8961−8980

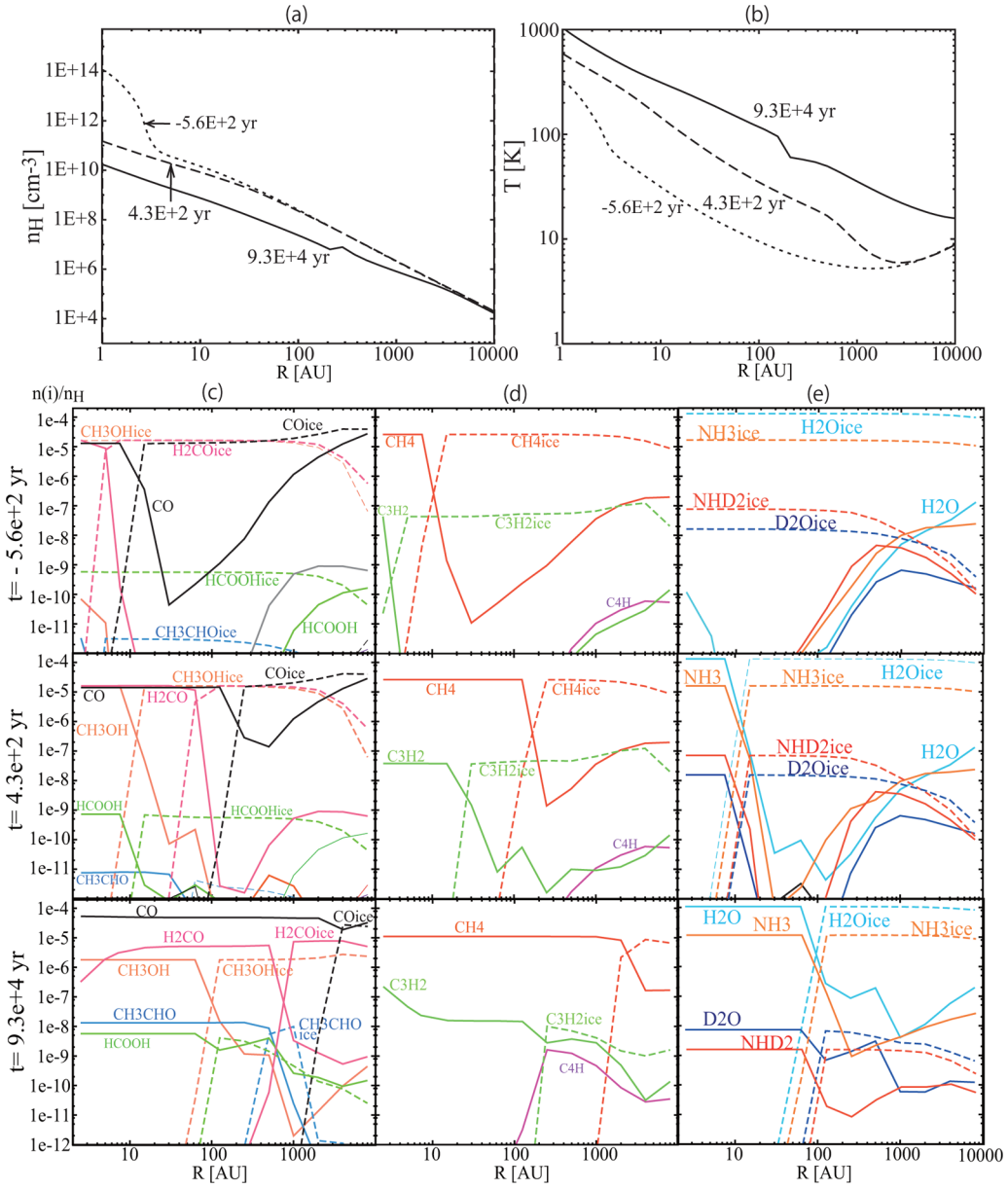

Figure 7. (a and b) Radial distribution of density and temperature in 1D radiation hydrodynamics model of star forming core by Masunaga et al.[188] and Masunaga and Inutsuka.[189] Three evolutionary stages are shown; the labels depict the time after the birth of the protostar. (c) Distribution of CO and COMs, (d) CH_4 and carbon chains, and (e) H_2O, NH_3, and their doubly deuterated isotopologues in the three evolutionary stages. Solid lines depict gas phase species, while the dashed lines depict ice. One astronomical unit (1 AU) corresponds to the distance between the Sun and Earth, 1.5×10^{13} cm. Figure adapted from ref 187 by permission of the AAS, copyright 2012.

protostellar evolution and (b) are there any other parameters (than the collapse time scale) which can be responsible for the chemical variation among protostellar cores?

With these questions in mind, Aikawa et al.[187] investigated molecular evolution in the core model of Masunaga et al.[188] and Masunaga and Inutsuka[189] using the gas-grain network model of Garrod and Herbst.[62] As described in the start of this section, the thermal structure of the core is very important in star formation, because temperature (together with gas density) determines the pressure gradient, which competes with gravity. To accurately evaluate the thermal structure in the evolving core, Masunaga et al.[188] and Masunaga and Inutsuka[189] simultaneously calculated the hydrodynamics and radiation transfer, which is called radiation hydrodynamics, in 1-dimensional (spherical) core. Figure 7a,b shows their radial distribution of density and temperature at assorted evolutionary stages. The initial condition is a cold molecular cloud core with the central density of $n(H_2) \approx 3 \times 10^4$ cm^{-3}, which is more realistic than the initial condition of the inside-out collapse. The core collapses to form a protostar in 2.5×10^5 yr. In Figure 7, $t = 0$ is defined as the moment of protostellar birth; that is, $t = -5.6 \times 10^2$ yr corresponds to the first core stage, in which we can see a hydrostatic core with the radius of a few AU. Dashed and solid lines in Figure 7a,b depict the density and temperature in the protostellar envelope, i.e., the gas around the protostellar, at $t = 4.3 \times 10^2$ yr and 9.3×10^4 yr after the protostar is born. The protostar itself is as small as $\sim 10^{-2}$ AU and thus is not plotted in Figure 7. The temperature in the envelope increases with time, although it remains low ($\leq$20 K)

dx.doi.org/10.1021/cr4003193 | Chem. Rev. 2013, 113, 8961−8980

in the outer radius $\geq 10^3$ AU. The envelope density decreases with time as the gas falls to the central protostar.

In the core model, chemical reactions proceed in infalling fluid parcels. Figure 6 schematically summarizes the evolution of the core structure and chemical processes in the three different temperature ranges along the flow. As a fluid parcel enters the warm regions, molecules sublimate from the ice mantle layer of dust grains. The sublimation radius moves outward as the core becomes hotter.[156] Sublimation of abundant molecule (e.g., CO) affects the gas phase chemistry significantly. For example, the dominant molecular ion changes with radius.[120,187]

Figure 7c shows radial distribution of CO and complex organic molecules (COMs) at the three time steps, at which the core structure is shown in Figure 7a,b. We can see that CO ice is abundant in the outer region in which the temperature is lower than the sublimation temperature of CO ∼20 K. The depletion factor of CO varies with radius. In the outer cold region, gaseous CO decreases inward, because the density increases and thus the adsorption time scale decreases (eq 11) inward. CO is sublimated to be abundant in the gas phase inside the sublimation radius, at which the temperature reaches ∼20 K. Such radial profile is derived also from molecular line observation of protostars and are called "drop-abundance profile".[176,190,191] The CO sublimation radius migrates outward as the core evolves and the core temperature rises. The peak CO depletion factor in a core declines as the core evolves, since the core density decreases with time. It is consistent with the observation by Jørgensen et al.,[175,176] who found the freeze-out zone decreases significantly with the core evolution. It is also notable that the CO abundance inside the sublimation radius is not necessarily equal to the canonical abundance. Specifically, in the early two evolutionary stages ($t = -5.6 \times 10^2$ and 4.3×10^2 yr) in Figure 7, CH_4 and CH_3OH are slightly more abundant than CO, and CO abundance is as low as 10^{-5}. Although CO abundance inside the sublimation radius gradually increases as the core evolves, it remains $\leq 2 \times 10^{-5}$ when the total luminosity of the core is $\leq$ a few $L_\odot$ in the model. Such low CO abundance is actually observed in protostellar cores.[191−193]

As the core evolves, COMs become more abundant, while CH_3OH decreases. The COMs are mainly formed by the grain surface reaction at $T \geq 30$ K [62]. Since such temperature region extends to outer radii as the core evolves, infalling fluid parcels experience COMs formation for a longer time scale in later stages.

Figure 7d shows radial distribution of CH_4 and carbon chains. At $t = 9.3 \times 10^4$ yr, WCCC is reproduced at $r \approx 2000$ AU; CH_4 is sublimated and the abundance of carbon chain species increases inward. In earlier stages, on the other hand, such a rise of carbon chains is not significant at the CH_4 sublimation radius. In the model, carbon chain formation starts with $C^+ + CH_4$ (reaction 6). In the early stages, the gas density at the CH_4 sublimation radius is too high for C^+ to be abundant. The model indicates that WCCC can not be significant in cores in which the gas density is $\sim 10^8$ cm^{-3} or higher at the sublimation radius of CH_4.

While the mass accretion rate onto the protostar changes rather continuously in the model described above,[189] observations of low-mass protostars indicate that the accretion could be episodic.[194,195] For a YSO embedded in cloud gas, the mass accretion rate estimated from the luminosity of the YSO is much lower than the mass of the object divided by the duration of the embedded phase, which indicate that a large fraction of mass accretes to the protostar in a time that is short compared to the duration of the embedded phase. Such bursts of mass accretion would heat the envelope, which then cools when the accretion rate diminishes. The temporal heating would release CO to gas phase, which could be observed for 10^3−10^4 yrs after the burst, and also could form pure CO_2 ice.[196,197] Effects of mass accretion bursts on other molecules remain to be explored.

6.4. Molecular D/H Ratio in Protostellar Cores

Figure 7e shows the distribution of H_2O, NH_3, and their deuterated analogues. At early stages (e.g., $t = -5.6 \times 10^2$ yr), the molecular D/H ratio is extremely enhanced by CO depletion in the outer radius $r > 100$ AU (section 5.2). The molecular abundances in the gas phase are, however, relatively low, because H_2O and NH_3 themselves are frozen onto grains, and because both NH_3 and H_2O are formed more efficiently by hydrogenation on grain surfaces than in the gas phase.

It should be noted that ice is also deuterated (section 5.2.). The recombination of H_3^+ and its deuterated isotopologues (reaction 22) enhances atomic D/H ratio in the gas phase, which propagates to ice mantle via adsorption onto grains and hydrogenation (Figure 4d,f; section 5). The molecular D/H ratio in ice mantle, however, is lower than the gas-phase D/H ratio in the CO depletion zone, since the ice has been accumulated all the way from the initial molecular cloud core stage, where CO depletion is not yet significant. In the central region, H_2O and NH_3 abundances in the gas phase are significantly increased by the sublimation, but the D/H ratios becomes lower than those in outer radius.

Figure 7e also shows that the D/H ratio of NH_3 inside the sublimation radius decreases as the core evolves. In early stages, a significant amount of multiply deuterated NH_3 is formed and frozen onto grains around the CO depletion zone, which then sublimates at the inner radius. In the latest stage ($t = 9.3 \times 10^4$ yr), the CO depletion is not significant to enhance the abundance of multiply deuterated NH_3. The model indicates that the molecular D/H ratio varies with the evolutionary stage of the cores. In observations, the beam size matters as well; if the beam size is much larger than the central sublimation zone, it probes the outer radius with low molecular abundance and high D/H, while the observation with very high spatial resolution can probe the central sublimation zone, where the gaseous molecules are abundant but the D/H ratio is lower than the outer radius.

Aikawa et al.[187] also investigated the D/H ratio of COMs and carbon chains in protostellar core. They found that COMs and carbon chains inherit the D/H ratio of their mother molecule, CH_3OH and CH_4, respectively. It should be noted that CH_3OH ice (and H_2CO ice) has additional Deuteration mechanism; the abstraction and substitution of H by D atom on grain surface, e.g., $CH_3OH + D \rightarrow CH_2OH + HD$ [198]. Taquet et al.[199] showed that these reactions can heavily deuterate H_2CO and CH_3OH at high densities ($n(H_2) \geq 10^6$ cm^{-3}), which can account for the extreme D/H ratio observed in some protostellar cores.[200]

6.5. 2D/3D Models

So far, we have reviewed a protostellar core model with spherical symmetry. However, in reality, cloud cores are rotating with angular velocity of $\omega \approx 10^{-14}$ s^{-1},[21] and the spherical symmetry breaks in the central regions as the collapse proceeds. Because of the angular momentum conservation, the

dx.doi.org/10.1021/cr4003193 | Chem. Rev. 2013, 113, 8961−8980

centrifugal force increases for infalling fluid parcels and eventually balances with the gravity at the centrifugal radius

$$r_{\rm cent} = \frac{(r^2\omega)_{\rm init}^{\ 2}}{GM_{\rm core}} \approx 400\left(\frac{r_{\rm init}}{0.1\ {\rm pc}}\right)^4\left(\frac{\omega_{\rm init}}{1\times10^{-14}\ {\rm s}^{-1}}\right)^2\left(\frac{1M_\odot}{M_{\rm core}}\right){\rm AU} \quad (23)$$

to form a circumstellar disk, where $M_{\rm core}$ and $r_{\rm init}$ are the mass and the initial radius of the core. The disk is of significant astronomical and chemical interest, because it is a formation site of planetary system. Outflows are also ejected in polar directions from the vicinity of the central protostar via the interaction of the rotating gas and magnetic fields. Figure 8 is a schematics view of structure around the protostar obtained by magneto-hydrodynamic simulations.[201]

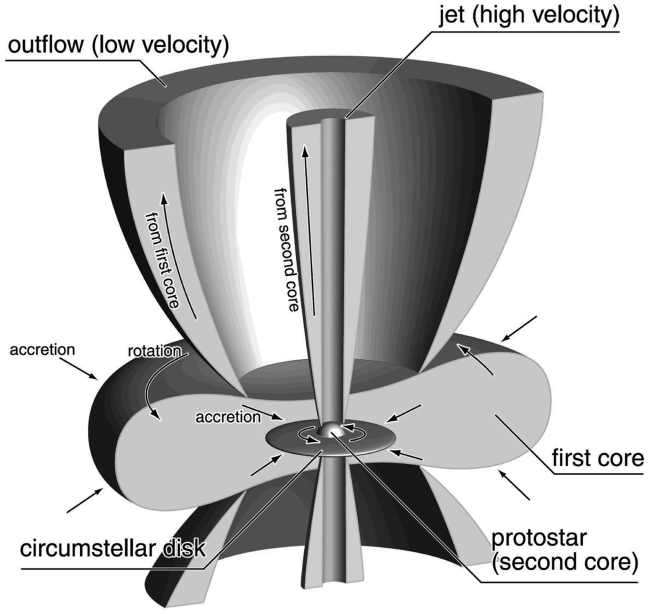

Figure 8. Physical structure in the vicinity of a new-born protostar. The protostar is still surrounded by the first core, which is ≤ several AU in size and will evolve to a protoplanetary disk.[208] A high velocity (∼30 km s^{-1}) jet and a low-velocity outlow (∼5 km s^{-1}) are ejected from the central region. Reproduced by permission of the AAS from ref 208, copyright 2008.

While the protoplanetary disks are ubiquitously observed around young stars, called Class II objects, which have already lost its envelope gas,[24] astronomers are currently trying to observe younger protostars (Class 0-I) to probe the disk formation processes. Rotation of circumstellar gas has been detected in several protostellar cores. Ohashi et al.,[202] for example, plotted specific angular momentum (angular momentum per unit mass of gas) of cloud cores as a function of their radius and found that inside ∼0.03 pc the specific angular momentum is constant; that is, the rotation velocity $v_{\rm rot}$ is inversely proportional to the radius, $r_{\rm rot} \propto r^{-1}$. Di Francesco et al.[173] detected rotational motion of gas around NGC1333 IRAS 4A, while another protostellar core in the system, NGC1333 IRAS 4B did not show rotation signature. The ultimate goal of these observations is to find a forming young disk, which is supported by the Keplerian rotation, i.e., $v_{\rm rot} \propto r^{1/2}$. Recently, the Kepler rotation of gas is found around young protostellar core L1527,[203] TMC-1A, and L1489 IRS.[204] Confirmation and more detailed analysis of these objects will be performed in near future.

Such nonspherical structure would have significant effects on molecular abundances. For example, in a spherical model, fluid parcels fall to the central star in a short time scale (∼100 yr), once they enter the region of $r \leq 100$ AU. In nonspherical core, on the other hand, fluid parcels enter the circumstellar disk and could stay around the protostar for a longer time scale, since the disk is supported by the rotation. We could thus expect more chemical reactions to proceed.[187] Chemistry in the 2D/3D model could also tell us the initial abundance of protoplanetary disk, and which molecular transition is the best to observationally trace the forming disk and foot point (and thus the driving mechanism) of the outflow.

Several groups have constructed a chemical model of 2D or 3D collapse. Visser et al.[205,206] constructed a 2D (axisymetric) model of disk formation from the inside-out collapse with rotation to protoplanetary disks by combining semianalytical models. The temperature distribution is calculated by solving radiation transfer assuming appropriate size and luminosity of the protostar. Outflow is not included in the model, but they set outflow cavities (vacant region where the gas is blown away by the outflow) in polar regions, through which the UV radiation from the protostar irradiate the cavity wall. Then they followed trajectories of infalling fluid parcels and solved chemical network of gas-phase reactions and hydrogenation reactions on grain surfaces along them, to obtain chemical history of fluid parcels that end up in the disk. They found that the fluid parcels in the disk have variety of chemical history depending on the trajectories. For example, the fluid parcel which goes through the region close to the outflow cavity experiences photodissociation, although some fluid parcels and species mainly experience evaporation and refreeze out only. Harsono et al.[209] recently calculated radiation transfer of this model to investigate which molecular line is suitable to trace the disk still embedded in the protostellar core.

van Weeren et al.[210] adopt the 2D hydrodynamic simulation of low-mass star formation by Yorke and Bodenheimer.[211] They investigate the trajectory of fluid parcels, along which the chemical reaction network is solved. The molecular abundances in the envelope show reasonable agreements with the observation by Jørgensen et al.[212]

Furuya et al.[207] and Hincelin at al.[213] investigated chemistry in a 3D radiation hydrodynamics model of star-forming core of Tomida et al.[214] and Commerçon et al.,[215] respectively. The models start from a cold prestellar core and evolves to the first core and its envelope. Since the initial core is rotating, the first core has a flattened disk-like structure (Figure 8). The model halts at the first core stage, since the radiation hydrodynamics calculation is very time-consuming. However, according to other hydrodynamic simulations, which do not include radiation transfer and thus are less time-consuming, the first core will evolve to the protoplanetary disk, together with the accreting gas from the envelope, after the protostar is formed.[208] Hence the chemistry in and around the first core is considered to be the initial condition of the protoplanetary disk. Figure 9a shows a trajectory of one fluid parcel in the model of Furuya et al.[207] In the envelope region, the trajectory is almost free-fall, until the parcel enters the first core, which has much higher density and temperature than the envelope region. Figure 9b shows the abundance of gaseous CH_3OH in the $x-z$ plane and the $x-y$ plane (the plane perpendicular to

dx.doi.org/10.1021/cr4003193 | Chem. Rev. 2013, 113, 8961−8980

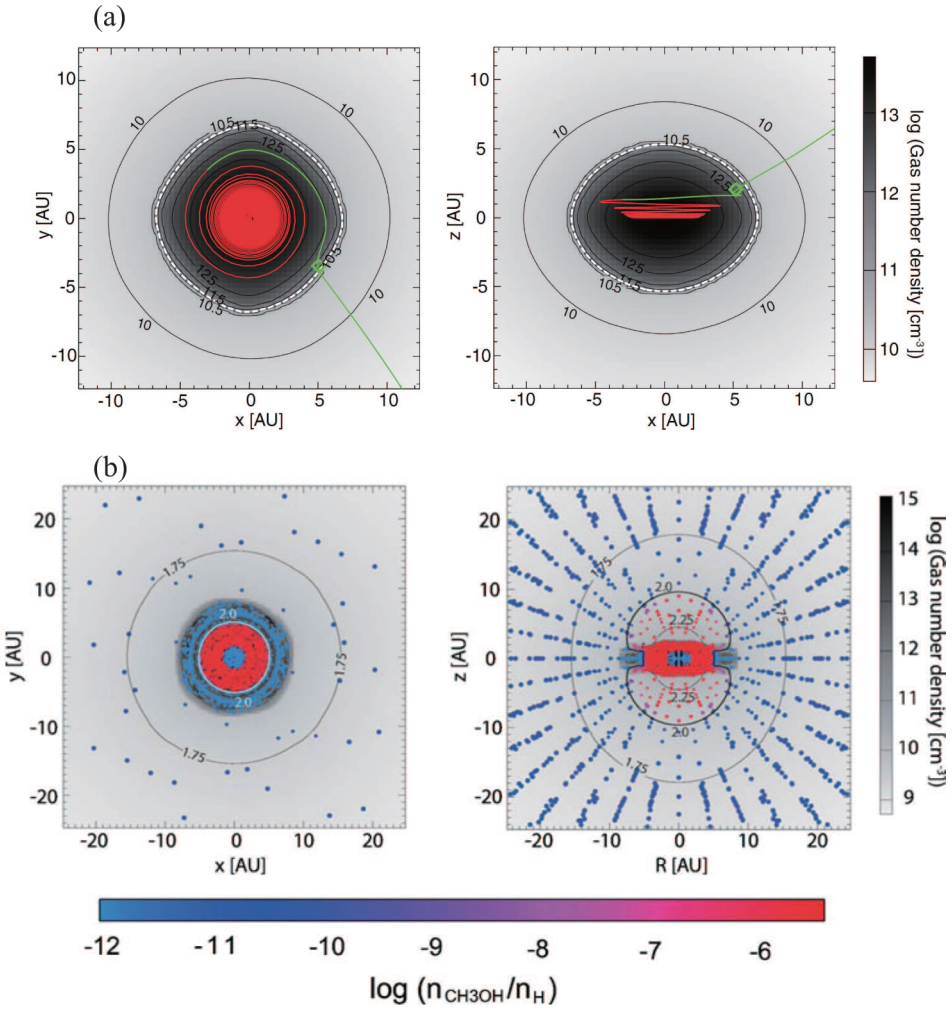

Figure 9. (a) Trajectories of a fluid parcel in the 3D radiation hydrodynamic model. The contours depict the density distribution. The $x-y$ plane is perpendicular to the rotation axis of the initial cloud core. (b) Spatial distribution of fluid parcels, which are color coded according to the abundance of gaseous CH_3OH. Figure adapted from ref 207 by permission of the AAS, copyright 2012.

the rotation axis) at 2800 years after the first core is formed. The CH_3OH distribution basically follows the temperature distribution; it is mainly formed in the cold prestellar stage and sublimated when the fluid parcels enter the region of $T > 100$ K. At the central region of the first core, CH_3OH is destroyed by the thermal dissociation. Grain-surface reactions among heavy element molecules are limited, because the size of the warm ($T \approx$ severel 10 K) envelope is still small in the first core stage. Yet the model shows that some COMs, such as CH_3OH and $HCOOCH_3$, are associated with the first core (<10 AU). Carbon chains, on the other hand, are formed at high temperature (>700 K).

7. FUTURE PROBLEMS

In the past decade, we have seen significant progresses in observation and modeling of prestellar cores and protostellar cores. Comprehensive view from prestellar core to protostellar core is now emerging in theoretical models and also by compilation of observations at various evolutionary stages.

There are still several remaining issues. First, theoretical models indicate that grain−surface reactions at several 10 K would be important for the formation of COMs, which are observed in hot corinos. Accurate formulation and modeling of grain surface reactions are, however, complicated, since the grain−surface reactions are stochastic. In rate equations, the rate of grain surface reaction is usually given by the product of migration rate, and number of reactants i and j on a grain. This formulation would be appropriate if there are many adsorbed molecules on grains. However, it overestimates the rate when the number of the adsorbed species i and j are less than unity per grain species i and j most probably exist on different dust grains and cannot react with each other.[216] When there are more than a monolayer of adsorbed species, we have another problem; it is not clear if all the adsorbed molecules can participate in the reaction. Molecules buried in deep ice layers may not easily migrate and react. There are currently many modeling methods of grain surface reactions, which are more detailed and sophisticated than rate equations.[199,217−219] These calculations are often more time-consuming, so the application to the hydrodynamic models are still limited. Recent detection of COMs in prestellar cores[220] indicates that the formation of COMs could be more efficient at ∼10 K than realized in the models. Recently, Vasyunin and Herbst[221] succeeded in producing these prestellar COMs via a sequence of gas-phase reactions between precursor species, which are formed on grains and then nonthermally desorbed to the gas phase.

Molecular isotope ratio of heavy elements, $^{13}C/^{12}C$, $^{15}N/^{14}N$, and $^{18}O/^{17}O/^{18}O$, in star-forming cores are of special interest in

dx.doi.org/10.1021/cr4003193 | Chem. Rev. 2013, 113, 8961−8980

relation to isotope anomalies detected in meteorites and interplanetary dust in our Solar system.[222] In molecular cloud chemistry, isotope fractionation of C, O, and N is known to occur via exothermic exchange reactions (e.g., $^{13}C^+ + {}^{12}CO \rightarrow {}^{12}C^+ + {}^{13}CO$) and UV shielding. Since CO, the major carrier of C and O, dissociates via predissociation and since its photodissociation wavelengths overwrap with those of H_2, self- and mutual-shielding is important. Self-shielding is less efficient for minor isotopologues (e.g., $^{12}C^{18}O$) and thus leads to isotope fractionation.[223] These fractionation mechanisms have been implemented to pseudotime dependent models,[224−227] but the application to collapsing star-forming cores is very limited.[228] Effect of o/p ratio of H_2 on N isotope ratio has recently been investigated in a pseudotime dependent model[229] of molecular clouds.

The chemistry in disk formation phase is not yet fully understood in theoretical models. Visser et al.[205,206] did not include COMs, while Furuya et al.[207] solved a large network model with COMs but reached up to the first core phase. It is also desirable to understand the effect of shock and outflows on chemistry. Lunine et al.[230] investigated sublimation of ice at the shock when the infalling material in the envelope enters the disk, while Ilee et al.[231] investigated molecular evolution in gravitationally unstable disk, in which spiral waves and shocks heat the disk material.

The central region of the protostellar core is yet to be investigated via high spatial resolution observations such as ALMA (atacama large millimeter and submillimeter array). The central warm region (≥100 K) of the protostellar core is as small as ≤100 AU and thus has been resolved only marginally. So far, the emission lines from protostellar cores are often spatially unresolved. The molecular abundances are thus estimated by assuming simple spherical core models with radial distributions of density and temperature; the derived abundances vary significantly depending on the assumed model. The spatial scale of 100 AU coincides with the centrifugal radius, i.e., a size of the disk, so it would be unlikely that the physical structure is spherical. ALMA is capable of spatially resolving the central region of the protostellar core with the resolution of ∼10 AU in nearby star-forming regions. Together with the combined models of hydrodynamics and chemistry, ALMA data will reveal how the protoplanetary disks are formed in young protostellar cores and how the interstellar matter evolves to planetary matter. Basic chemical and physical data of molecules, such as spectroscopic data,[232,233] collisional cross section to excite molecules to various energy states,[234] and rate and branching ratio of chemical reactions both in the gas phase[32] and grain surfaces[61] are vital for the assignment of lines observed by ALMA and improvement of models.

AUTHOR INFORMATION

Corresponding Author

*E-mail: aikawa@kobe-u.ac.jp.

Notes

The authors declare no competing financial interest.

Biography

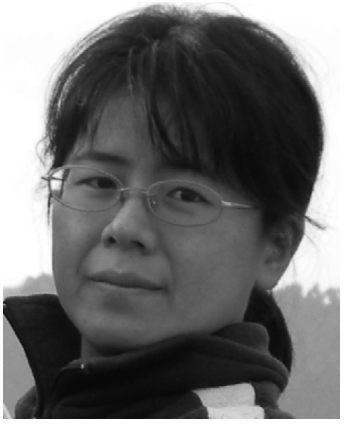

Yuri Aikawa received her Ph.D. at University of Tokyo in March 1998. She worked with Prof. Eric Herbst at The Ohio State University as a JSPS postdoctoral fellow (research abroad) in 1998−2000 and then worked with Prof. Satoshi Yamamoto for one month at University of Tokyo as a JSPS postdoctoral fellow. She spent 8 years at Kobe University as an assistant professor. She is an associate professor of Earth and Planetary Science at Kobe University since 2008.

ACKNOWLEDGMENTS

The author thank the anonymous referees for useful comments to improve the manuscript. This study is supported by Grant-in-Aid for Scientific Research (C) 23540266 and Grant-in-Aid for Scientific Research on Innovative Areas 23103004.

REFERENCES

(1) Grevesse, N.; Noels, A.; Sauval, A. J. In *Cosmic Abundances*; Holt, S. S., Sonneborn, G. Eds.; ASP Conference Series; Astronomical Society of the Pacific: San Francisco, 1996; Vol. *99*, p 117.
(2) Gies, D. R.; Lambert, D. L. *Astrophys. J.* **1992**, *387*, 673.
(3) Asplund, M.; Grevesse, N.; Sauval, A. J.; Scott, P. *Annu. Rev. Astron. Astr.* **2009**, *47*, 481.
(4) Draine, B. T. *Annu. Rev. Astron. Astr.* **2003**, *41*, 241.
(5) Tielens, A. G. G. M. *The Physics and Chemistry of the Interstellar Medium*; Cambridge University Press: Cambridge, 2005; p 228.
(6) Tielens, A. G. G. M. *The Physics and Chemistry of the Interstellar Medium*; Cambridge University Press: Cambridge, 2005; p 351.
(7) Alves, J. F.; Lada, C. J.; Lada, E. A. *Nature* **2001**, *409*, 159.
(8) Tobin, J. J.; Hartman, L.; Valvet, N.; D'Alessio, P. *Astrophys. J.* **2008**, *679*, 1364.
(9) Irvine, W. M.; Goldsmith, P.; Hjalmarson, A., In *Interstellar Processes*; Hollenbach, D. J., Thronson, H. A. Jr., Eds.; D. Reidel Publishing Company: Dordrecht, Holland, 1987; p 561.
(10) Guelin, M.; Friberg, P.; Mezaoui, A. *Astron. Astrophys.* **1982**, *109*, 23.
(11) Geballe, T. R.; Oka, T. *Nature* **1996**, *384*, 334.
(12) McCarthy, M. C.; Gottliebm, C. A.; Gupta, H.; Thaddeus, P. *Astrophys. J. Lett.* **2006**, *652*, 141.
(13) Oka, T. *Phys. Rev. Lett.* **1980**, *45*, 531.
(14) Wilson, S.; Green, S. *Astrophys. J. Lett.* **1977**, *212*, 87.
(15) Ward-Thompson, D.; André, P.; Crutcher, R.; Johnstone, D.; Onishi, T.; Wilson, C. In *Protostars amd Planets V*; Reipurth, B., Jewit, D., Keil, K., Eds.; University of Arizona Press: Tucson, AZ, 2007; p 33.
(16) Shu, F. H.; Adams, F. C.; Lizano, S. *Annu. Rev. Astron. Astr.* **1987**, *25*, 23.
(17) Bergin, E. A.; Tafalla, M. *Annu. Rev. Astron. Astr.* **2007**, *45*, 339.
(18) di Francesco, J.; Evans, N. J., II.; Caselli, P.; Myers, P. C.; Shirley, Y.; Aikawa, Y.; Tafalla, M. In *Protostars and Planets V*; Reipurth, B., Jewit, D.,; Keil, K., Eds.; University of Arizona Press: Tucson, AZ, 2007; p 17.

(19) van Dishoeck, E. F.; Blake, G. A. *Annu. Rev. Astron. Astr.* **1998**, *36*, 317.
(20) Hayashi, C.; Nakazawa, K.; Nakagawa, Y. In *Protostars and Planets II*; Black, D. C., Matthews, M. S., Eds.; University of Arizona Press: Tucson, AZ, 1985; p 1100.
(21) Goodman, A. A.; Benson, P. J.; Fuller, G. A.; Myers, P. C. *Astrophys. J.* **1993**, *406*, 528.
(22) Beckwith, S. V. W.; Sargent, A. I.; Chini, R. S.; Güsten, R. *Astron. J.* **1990**, *99*, 924.
(23) Hartmann, L. *Accretion Processes in Star Formation*; Cambridge University Press: Cambridge, U.K., 1998; p 50.
(24) Williams, J. P.; Cieza, A. *Annu. Rev. Astron. Astr.* **2011**, *49*, 67.
(25) Dutrey, A.; Guilloteau, S.; Guelin, M. *Astron. Astrophys.* **1997**, *317*, 55.
(26) Bergin, E. A.; Aikawa, Y.; van Dishoeck, E. F.; Blake, G. A. In *Protostars and Planets V*; Reipurth, B., Jewit, D., Keil, K., Eds.; University of Arizona Press: Tucson, AZ, 2007; p 751.
(27) Terada, H.; Tokunaga, A. T.; Kobayashi, N.; Takato, N.; Hayano, Y.; Takami, H. *Astrophys. J.* **2007**, *667*, 303.
(28) Henning, Th.; Semenov, D. *Chem. Rev.* **2013**, this volume
(29) van Dishoeck, E. F.; Herbst, E.; Neufeld, D. A. *Chem. Rev.* **2013**, this volume
(30) Garrod, R. T.; Weaver, S. L. W.; Herbst, E. *Astrophys. J.* **2008**, *682*, 283.
(31) McElroy, D.; Walsh, C.; Markwick, A. J.; Cordiner, M. A.; Smith, K.; Millar, T. J. *Astron. Astrophys.* **2013**, *550*, 36.
(32) Wakelam.; et al. *Astrophys. J. Suppl. S* **2012**, *199*, 21.
(33) Baulch, D. L.; Bowman, C. T.; Cobos, C. T.; Cox, R. A.; Hust, Th.; Lerr, J. A.; Pilling, M. J.; Stocker, D.; Troe, J.; Tsang, W.; Walker, R. W.; Warnatz, J. *J. Phys. Chem. Ref. Data* **2005**, *34*, 757.
(34) Sims, I. *Astrochemistry: Recent Successes and Current Challenges*; Lis, D. C., Blake, G. A., Herbst, E., Eds.; Cambridge University Press: Canbridge, U.K., 2005; p 97.
(35) Dukey, W. W.; Williams, D. A. *Interstellar Chemistry*; Academic Press: London, 1984.
(36) Tielens, A. G. G. M., *The Physics and Chemistry of the Interstellar Medium*; Cambridge University Press: Cambridge, U.K., 2005; p 348.
(37) Dalgarno, A. *Proc. Natl Acad. Sci.* **2006**, *103*, 12269.
(38) Milligan, D. B.; McEwan, M. *Chem. Phys. Lett.* **2000**, *319*, 482.
(39) Klippenstein, S. J.; Georgievskii, Y.; McCall, B. J. *J. Phys. Chem.* **2010**, *114*, 278.
(40) Jensen, M. J.; Bilodeau, R. C.; Safvan, C. P.; Andersen, L. H.; Pedersen, H. B.; Heber, O. *Astrophys. J.* **2000**, *543*, 764.
(41) Barlow, S. E.; Dunn, G. H.; Schauer, M. *Phys. Rev. Lett.* **1984**, *52*, 902.
(42) Barlow, S. E.; Dunn, G. H.; Schauer, K. *Phys. Rev. Lett.* **1984**, *53*, 1610.
(43) Gerlich, D. *Phys. Scr.* **1995**, *59*, 256.
(44) Martinez, O., Jr.; Betts, N. B.; Villano, S. M.; Eyet, N.; Snow, T. P.; Bierbaum, V. M. *Astrophys. J.* **2008**, *686*, 1486.
(45) Herbst, E.; DeFrees, M. A.; Maclean, A. D. *Astrophys. J.* **1987**, *321*, 898.
(46) Bettens, R. P. A.; Collins, M. A. *J. Chem. Phys.* **1998**, *109*, 9728.
(47) Edvardsson, D.; Williams, C. F.; Clary, D. C. *Chem. Phys. Lett.* **2006**, *431*, 261.
(48) Jorfi, M.; Honvault, P.; Halvick, P. *Chem. Phys. Lett.* **2009**, *471*, 65.
(49) Bergeat, A.; Daranlot, J.; Hickson, K. M.; Costesm, M. *EAS Publ. Ser.* **2012**, *58*, 283.
(50) Williams, D. In *Dust and Chemistry in Astronomy*; Millar, T. J., Williams, D., Eds.; Institute of Physics Publishing: Philadelphia, PA, 1993; p 143.
(51) Watanabe, N.; Shiraki, T.; Kouchi, A. *Astrophys. J. Lett.* **2003**, *588*, L121.
(52) Chaabouni, H.; Bergeron, H.; Baouche, S.; Dulieu, F.; Matar, E.; Congiu, E.; Gavilan, L.; Lemaire, J. L. *Astron. Astrophys.* **2012**, *538*, 128.
(53) Katz, G. J.; Furman, I.; Biham, O.; Pirronello, V.; Vidali, G. *Astrophys. J.* **1999**, *522*, 305.
(54) Hiraoka, K.; Miyagoshi, T.; Takayama, T.; Yamamoto, K.; Kihara, Y. *Astrophs. J.* **1998**, *498*, 710.
(55) Dulieu, F.; Amiaud, L.; Congiu, E.; Fillion, J.-H.; Matar, E.; Memeni, A.; Pirronello, V.; Lemaire, J. L. *Astron. Astrophys.* **2010**, *512*, A30.
(56) Jing, D.; He, J.; Brucato, J.; De Sio, A.; Tozzetti, L.; Vidali, G. *Astrophys. J.* **2011**, *741*, L9.
(57) Whittet, D. C. B. In *Dust and Chemistry in Astronomy*; Millar, T. J., Williams, D., Eds; Institute of Physics Publishing: Philadelphia, PA, 1993; p 9.
(58) Hidaka, H.; Watanabe, M.; Kouchi, A.; Watanabe, N. *Phys. Chem. Chem. Phys.* **2011**, *13*, 15798.
(59) Watanabe, N.; Kouchi, A. *Astrophys. J. Lett.* **2002**, *57*, 173.
(60) Fuchs, G. W.; Cuppen, H. M.; Ioppolo, S.; Romanzin, C.; Bisschop, S. E.; Andersson, S.; van Dishoeck, E. F.; Linnartz, H. *Astron. Astrophys.* **2009**, *505*, 629.
(61) Watanabe, N.; Kouchi, A. *Prog. Surf. Sci.* **2008**, *83*, 439.
(62) Garrod, R. T.; Herbst, E. *Astron. Astrophys.* **2006**, *457*, 927.
(63) Herbst, E.; van Dishoeck, E. F. *Annu. Rev. Astron. Astrophys.* **2009**, *47*, 427.
(64) Leger, A.; Jura, M.; Omont, A. *Astron. Astrophys.* **1985**, *144*, 147.
(65) Hasegawa, T.; Herbst, E. *Mon. Not. R. Astron. Soc.* **1993**, *261*, 83.
(66) Andersson, S.; van Dishoeck, E. F. *Astron. Astrophys.* **2008**, *491*, 907.
(67) Öberg, K. I.; Linnartz, H.; Visser, R.; van Dishoeck, E. F. *Astrophys. J.* **2009**, *693*, 1209.
(68) Öberg, K. I.; van Dishoeck, E. F.; Linnartz, H. *Astron. Astrophys.* **2009**, *496*, 281.
(69) Muñz Caro, G. M.; Jimenez-Escobar, A.; Martin-Gago, J. A.; Rogero, C.; Atienza, C.; Puertas, S.; Sobrado, J. M.; Torres-Redondo, J. *Astron. Astrophys.* **2010**, *522*, 108.
(70) Arasa, C.; Andersson, S.; Cuppen, H. M.; van Dishoeck, E. F.; Kroes, G. J. *J. Chem. Phys.* **2011**, *134*, 164503.
(71) Takahashi, J.; Masuda, K.; Nagaoka, M. *Astrophys. J.* **1999**, *520*, 724.
(72) Goumans, T. P. M.; Richard, C.; Catlow, A.; Brown, W. A. *Mon. Not. R. Astron. Soc.* **2009**, *393*, 1403.
(73) Willacy, K.; Millar, T. J. *Mon. Not. R. Astron. Soc.* **1998**, *298*, 562.
(74) Tielens, A. G. G. M. *The Physics and Chemistry of the Interstellar Medium*; Cambridge University Press: Cambridge, U.K., 2005; p 241.
(75) van Dishoeck, E. F. In *Rate Coefficients in Astrochemistry*; Millar, T. J., Williams, D. A., Eds.; Springer: Nerherlands, 1988; p 49.
(76) Draine, B. T.; Bertoldi, F. *Astrophys. J.* **1996**, *468*, 269.
(77) Bergin, E. A.; Hartmann, L. W.; Raymond, J. C.; Ballesteros-Paredes, J. *Astrophys. J.* **2004**, *612*, 921.
(78) Suzuki, H.; Yamamoto, S.; Ohishi, M.; Kaifu, N.; Ishikawa, S. I.; Hirahara, Y.; Takano, S. *Astrophys. J.* **1992**, *392*, 551.
(79) Hirahara, Y.; Suzuki, H.; Yamamoto, S.; Kawaguchi, K.; Kaifu, N.; Ohishi, M.; Takano, S.; Ishikawa, S. I.; Masuda, A. *Astrophys. J.* **1992**, *394*, 539.
(80) Bergin, E. A.; Neufeld, D. A.; Melnick, G. J. *Astrophys. J. Lett.* **1999**, *510*, 145.
(81) Hassel, G. E.; Herbst, E.; Bergin, E. A. *Astron. Astrophys.* **2010**, *515*, 66.
(82) Inoue, T.; Inutsuka, S. *Astrophys. J.* **2012**, *759*, 35.
(83) André, Ph.; Men'shchikov, A.; Bontemps, S.; Könyves, V.; Motte, F.; Schneider, N.; Didelon, P.; Minier, V.; Saraceno, P.; Ward-Thompson, D.; di Francesco, J.; White, G.; Molinari, S.; Testi, L.; Abergel, A.; Griffin, M.; Henning, Th.; Royer, P.; Merín, B.; Vavrek, R.; Attard, M.; Arzoumanian, D.; Wilson, C. D.; Ade, P.; Aussel, H.; Baluteau, J.-P.; Benedettini, M.; Bernard, J.-Ph.; Blommaert, J. A. D. L.; CambrÃl'sy, L.; Cox, P.; di Giorgio, A.; Hargrave, P.; Hennemann, M.; Huang, M.; Kirk, J.; Krause, O.; Launhardt, R.; Leeks, S.; Le Pennec, J.; Li, J. Z.; Martin, P. G.; Maury, A.; Olofsson, G.; Omont, A.; Peretto, N.; Pezzuto, S.; Prusti, T.; Roussel, H.; Russeil, D.; Sauvage, M.; Sibthorpe, B.; Sicilia-Aguilar, A.; Spinoglio, L.; Waelkens, C.; Woodcraft, A.; Zavagno, A. *Astron. Astrophys. Lett.* **2010**, *518*, 102.
(84) Arzoumanian, D.; André, P.; Didelon, P.; Könyves, V.; Schneider, N.; Men'shchikov, A.; Sousbie, T.; Zavagno, A.;

Bontemps, S.; di Francesco, J.; Griffin, M.; Hennenmenn, M.; Hill, T.; Kirk, J.; Martin, P.; Minier, V.; Molinari, S.; Motte, F.; Peretto, N.; Pezzuto, S.; Spinoglio, L.; Ward-Thompson, D.; White, G.; Wilson, C. D. *Astron. Astrophys.* **2011**, *529*, L6.
(85) Palmeirim, P.; André, Ph.; Kirk, J.; Ward-Thompson, D.; Arzoumanian, D.; Könyves, V.; Didelon, P.; Schneider, N.; Benedettini, M.; Bontemps, S.; Di Francesco, J.; Elia, D.; Griffin, M.; Hennemann, M.; Hill, T.; Martin, P. G.; Men'shchikov, A.; Molinari, S.; Motte, F.; Nguyen Luong, Q.; Nutter, D.; Peretto, N.; Pezzuto, S.; Roy, A.; Rygl, K. L. J.; Spinoglio, L.; White, G. L. *Astron. Astrophs.* **2013**, *550*, 38.
(86) Millar, T. J.; Farquhar, P. R. A.; Willacy, K. *Astron. Astrophys. Suppl. S* **1997**, *121*, 139.
(87) Terzieva, R.; Herbst, E. *Astrophys. J.* **1998**, *501*, 207.
(88) Hincelin, U.; Wakelam, V.; Hersabt, F.; Guilloteau, S.; Loison, J. C.; Honvault, P.; Troe, J. *Astron. Astrophys.* **2011**, *530*, 61.
(89) Pratap, P.; Dickens, J. E.; Snell, R. L.; Miralles, M. P.; Bergin, E. A.; Irvine, W. M.; Schloerb, F. P. *Astrophys. J.* **1997**, *486*, 862.
(90) Kaifu, N.; Ohishi, M.; Kawaguchi, K.; Saito, S.; Yamamoto, S.; Miyaji, T.; Miyazawa, K.; Ishikawa, S.; Noumaru, C.; Harasawa, S.; Okuda, M.; Suzuki, H. *Pub. Astron. Soc. Jpn.* **2004**, *56*, 69.
(91) Stancil, P. C.; Lepp, S.; Dalgarno, A. *Astrophys. J.* **1998**, *509*, 1.
(92) Nakamura, F.; Umemura, M. *Astrophys. J.* **2001**, *548*, 19.
(93) Abel, T.; Bryan, G. L.; Norman, M. L. *Science* **2002**, *295*, 93.
(94) Galli, D.; Palla, F. *Annu. Rev. Astron. Astrophys.* **2013**, *51*, 163.
(95) Shull, J. M.; Draine, B. T. *Interstellar Processes*; Hollenbach, D. J., Thronson, H. A., Jr., Eds.; D. Reidel Publishing Company: Dordrecht, The Netherlands, 1987; p 283.
(96) Landau, L. D.; Lifshitz, E. M. *Fluid Mechanics*; Pergamon Press: Oxford, U.K., 1987; p 313.
(97) Wolfire, M. G.; Hollenbach, D.; McKee, C. F.; Tielens, A. G. G. M.; Bakes, E. L. O. *Astrophys. J.* **1995**, *443*, 152.
(98) Koyama, H.; Inutsuka, S. *Astrophys. J.* **2000**, *532*, 980.
(99) Hollenbach, D.; McKee, C. F. *Astrophys. J. Suppl. S.* **1979**, *41*, 555.
(100) Draine, B. T.; Roberge, W. G.; Dalgarno, A. *Astrophys. J.* **1983**, *264*, 485.
(101) Kaufman, M. J.; Neufeld, D. A. *Astrophys. J.* **1996**, *456*, 611.
(102) Hartmann, L. *Accretion Processes in Star Formation*; Cambridge University Press: Cambridge, U.K., 1998; p 35.
(103) Tafalla, M.; Myers, P. C.; Caselli, P.; Walmsley, C. M.; Comito, C. *Astrophys. J.* **2002**, *569*, 815.
(104) Hirota, T.; Ito, T.; Yamamoto, S. *Astrophys. J.* **2002**, *565*, 359.
(105) de Geus, E.; de Zeeuw, P.; Lub, J. *Astron. Astrophys.* **1989**, *216*, 44.
(106) Bonnor, W. B. *Mon. Not. R. Astron. Soc.* **1956**, *116*, 351.
(107) Kandori, R.; Nakajima, Y.; Tamura, M.; Tatematsu, K.; Aikawa, Y.; Naoi, T.; Sugitani, K.; Nakaya, H.; Nagayama, T.; Nagata, T.; Kurita, M.; Kato, D.; Nagashima, C.; Sato, S. *Astron. J.* **2005**, *130*, 2166.
(108) Caselli, P.; Walmsley, C. M.; Zucconi, A.; Tafalla, M.; Dore, L.; Myers, P. C. *Astrophys. J.* **2002**, *565*, 331.
(109) Crapsi, A.; Caselli, P.; Walmsley, C. M.; Myers, P. C.; Tafalla, M.; Lee, C. W.; Bourke, T. L. *Astrophys. J.* **2005**, *619*, 379.
(110) Kirk, H.; Johnstone, D.; Tafalla, M. *Astrophys. J.* **2007**, *668*, 1042.
(111) Ciolek, G. E.; Basu, S. *Astrophys. J.* **2000**, *529*, 925.
(112) Crutcher, R. M. *Annu. Rev. Astron. Astrophys.* **2012**, *50*, 29.
(113) Keto, E.; Caselli, P. *Astrophys. J.* **2008**, *683*, 238.
(114) Aikawa, Y.; Herbst, E.; Roberts, H.; Caselli, P. *Astrophys. J.* **2005**, *620*, 330.
(115) Bergin, E. A.; Alves, J.; Huard, T.; Lada, C. J. *Astrophys. J. Lett.* **2002**, *570*, 101.
(116) Ceccarelli, C.; Caselli, P.; Herbst, E.; Tielens, A. G. G. M.; Caux, E. In *Protostars and Planets V*; Reipurth, B., Jewit, D., Keil, K., Eds.; University of Arizona Press: Tucson, AZ, 2007; p 47.
(117) Aikawa, Y.; Ohashi, N.; Inutsuka, S.; Herbst, E.; Takakuwa, S. *Astrophys. J.* **2001**, *552*, 639.
(118) Maret, S.; Bergin, E. A.; Lada, C. J. *Nature* **2006**, *442*, 425.
(119) Pagani, L.; Bourgoin, A.; Lique, F. *Astron. Astrophys.* **2012**, *548*, L4.
(120) Lee, J. E.; Bergin, E. A.; Evans, N. J., II *Astrophys. J.* **2004**, *617*, 360.
(121) Mathis, J. S.; Rumpl, W.; Nordsieck, K. H. *Astrophys. J.* **1977**, *217*, 425.
(122) Weingartner, J. C.; Draine, B. T. *Astrophys. J.* **2001**, *548*, 296.
(123) Acharyya, K.; Hassel, G. E.; Herbst, E. *Astrophys. J.* **2011**, *732*, 73.
(124) Flower, D. R.; Pineau des Forets, G.; Walmsley, C. M. *Astron. Astrophys.* **2005**, *436*, 933.
(125) Linsky, J. L. *Space Sci. Rev.* **2003**, *106*, 49.
(126) Hirota, T.; Ikeda, M.; Yamamoto, S. *Astrophys. J.* **2003**, *594*, 859.
(127) Millar, T. J.; Bennett, A.; Herbst, E. *Astrophys. J.* **1989**, *340*, 906.
(128) Roberts, H.; Herbst, E.; Millar, T. J. *Astron. Astrophys.* **2004**, *424*, 905.
(129) Smith, D.; Adams, N. G.; Alge, E. *Astrophys. J.* **1982**, *263*, 123.
(130) Vastel, C.; Caselli, P.; Ceccarelli, C.; Phillips, T.; Wiedner, M. C.; Peng, R.; Houde, M.; Dominik, C. *Astrophys. J.* **2006**, *645*, 1198.
(131) Caselli, P.; Vastel, C.; Ceccarelli, C.; van der Tak, F. F. S.; Crapsi, A.; Bacmann, A. *Astron. Astrophys.* **2008**, *492*, 703.
(132) Flower, D. R.; Pineau des Forêts, G.; Walmsley, C. M. *Astron. Astrophys.* **2006**, *449*, 621.
(133) Tafalla, M.; Santiago, J. *Astron. Astrophys.* **2004**, *414*, L53.
(134) Ford, A. B.; Yancy, S. L. *Astrophys. J.* **2011**, *728*, 144.
(135) Li, Z. Y.; Shematovich, V. I.; Wiebe, D. S.; Shustov, B. M. *Astrophys. J.* **2002**, *569*, 792.
(136) Lee, E. J.; Evans, N. J., II.; Shirley, Y. L.; Tatematsu, K. *Astrophys. J.* **2003**, *583*, 789.
(137) Tafalla, M.; Myers, P. C.; Caselli, P.; Walmsley, C. M. *Astron. Astrophys.* **2004**, *416*, 191.
(138) Tassis, K.; Willacy, K.; Yorke, H.; Turner, N. J. *Astrophys. J.* **2012**, *753*, 29.
(139) Tassis, K.; Willacy, K.; Yorke, H.; Turner, N. J. *Astrophys. J.* **2012**, *754*, 6.
(140) Larson, R. B. *Mon. Not. R. Astron. Soc.* **1969**, *145*, 271.
(141) Millar, T. J. In *Dust and Chemistry in Astronomy*; Millar, T. J., Williams, D., Eds.; Institute of Physics Publishing: Philadelphia, PA, 1993; p 249.
(142) Kurtz, S.; Casaroni, R.; Churchwell, E.; Hofner, P.; Walmsley, M. C. In *Protostars and Planets IV*; Mannings, V., Boss, A. P., Russell, S. S., Eds.; University of Arizona Press: Tucson, AZ, 2000; p 299.
(143) Sweitzer, J. S. *Astrophys. J.* **1978**, *225*, 116.
(144) Blake, G. A.; Sutton, E. C.; Masson, C. R.; Phillips, T. G. *Astrophs. J. Suppl.* **1986**, *60*, 357.
(145) Blake, G. A.; Sutton, E. C.; Masson, C. R.; Phillips, T. G. *Astrophys. J.* **1987**, *315*, 621.
(146) Walmsley, C. M.; Hermsen, W.; Henkel, C.; Mauersberger, R.; Wilson, T. L. *Astron. Astrophys.* **1987**, *172*, 311.
(147) Brown, P. D.; Charnley, S. B.; Millar, T. J. *Mon. Not. R. Astron. Soc.* **1988**, *231*, 409.
(148) Charnley, S. B.; Tielens, A. G. G. M.; Millar, T. J. *Astrophys. J. Lett.* **1992**, *399*, 71.
(149) Rodgers, S. D.; Charnley, S. B. *Astrophys, J.* **2001**, *546*, 324.
(150) Charnley, S. B. *Astrophys. J.* **1997**, *481*, 396.
(151) Doty, S. D.; van Dishoeck, E. F.; van der Tak, F. F. S.; Boonman, A. M. S. *Astron. Astrophys.* **2002**, *389*, 446.
(152) Nomura, H.; Millar, T. J. *Astron. Astrophys.* **2004**, *414*, 409.
(153) van der Tak, F. F. S.; van Dishoeck, E. F.; Evans, N. J., II; Bakker, E. J.; Blake, G. A. *Astrophys. J.* **1999**, *522*, 991.
(154) van der Tak, F. F. S.; van Dishoeck, E. F.; Evans, N. J., II; Bakker, E. J.; Blake, G. A. *Astrophys. J.* **2000**, *537*, 283.
(155) Ceccarelli, C.; Hollenbach, D. J.; Tielens, A. G. G. M. *Astrophys. J.* **1996**, *471*, 400.
(156) Rodgers, S. D.; Charnley, S. B. *Astrophys. J.* **2003**, *585*, 355.
(157) Shu, F. *Astrophys. J.* **1977**, *214*, 488.
(158) Adams, F. C.; Shu, F. H. *Astrophys. J.* **1985**, *296*, 655.

(159) Blake, G. A.; van Dishoeck, E. F.; Jansen, D. J.; Groesceck, T. D.; Mundy, L. G. *Astrophys. J.* **1994**, *428*, 680.
(160) van Dishoeck, E. F.; Blake, G. A.; Jansen, D. J.; Groesbeck, T. D. *Astrophys. J.* **1995**, *447*, 760.
(161) Blake, G. A.; Sandell, G.; van Dishoeck, E. F.; Groesbeck, T. D.; Mundy, L. G.; Aspin, C. *Astrophys. J.* **1995**, *441*, 689.
(162) Schöier, F. L.; Jørgensen, J. K.; van Dishoeck, E. F.; Blake, G. A. *Astron. Astrophys.* **2002**, *390*, 1001.
(163) Cazaux, E.; Tielens, A. G. G. M.; Ceccarelli, C.; Castets, A.; Wakelam, V.; Caux, E.; Parise, B.; Teyssier, D. *Astrophys. J.* **2003**, *593*, L51.
(164) Maret, S.; Ceccarelli, C.; Caux, E.; Tielens, A. G. G. M.; Jørgensen, J. K.; van Dishoeck, E. F.; Bacmann, A.; Castets, A.; Lefloch, B.; Loinard, L.; Parise, B.; Schöier, F. L. *Astron. Astrophys.* **2004**, *416*, 577.
(165) Kuan, Y.-J.; Huang, H.-C.; Charnley, S. B.; Hirano, N.; Takakuwa, S.; Wilner, D. J.; Liu, S.-Y.; Ohashi, N.; Bourke, T. L.; Qi, C.; Zhang, Q. *Astrophys. J.* **2004**, *616*, 27.
(166) Chandler, C. J.; Brogen, C. L.; Shirley, Y. L.; Loinard, L. *Astrophys. J.* **2005**, *632*, 371.
(167) Maret, S.; Ceccarelli, C.; Tielens, A. G. G. M.; Caux, E.; Lefloch, B.; Faure, A.; Castet, A.; Flower, D. R. *Astron. Astrophys.* **2005**, *442*, 527.
(168) Sakai, N.; Sakai, T.; Hirota, T.; Yamamoto, S. *Astrophys. J.* **2008**, *672*, 371.
(169) Caux, E.; Kahane, C.; Castets, A.; Coutens, A.; Ceccarelli, C.; Bacmann, A.; Bisschop, S.; Bottinelli, S.; Comito, C.; Helmich, F. P.; Lefloch, B.; Parise, B.; Schilke, P.; Tielens, A. G. G. M.; van Dishoeck, E.; Vastel, C.; Wakelam, V.; Walters, A. *Astron. Astrophys.* **2011**, *532*, 23.
(170) Coutens, A.; Vastel, C.; Caux, E.; Ceccarelli, C.; Bottinelli, S.; Wiesenfeld, L.; Faure, A.; Scribano, Y.; Kahane, C. *Astron. Astrophys.* **2012**, *539*, 132.
(171) Kahane, C.; Ceccarelli, C.; Faure, A.; Caux, E. *Astrophys. J.* **2013**, *763*, 38.
(172) Coutens, A.; Vastel, C.; Cazaux, S.; Bottinelli, S.; Caux, E.; Ceccarelli, C.; Demyk, K.; Taquet, V.; Wakelam, V. *Astron. Astrophys.* **2013**, *553*, 75.
(173) Di Francesco, J.; Myers, P. C.; Wilner, D. J.; Ohashi, N.; Mardones, D. *Astrophys. J.* **2001**, *562*, 770.
(174) Boogert, A. C. A.; Hogerheijde, M. R.; Blake, G. A. *Astrophys. J.* **2002**, *568*, 761.
(175) Jørgensen, J. K.; Schöier, F. L.; van Dishoeck, E. F. *Astron. Astrophys.* **2002**, *389*, 908.
(176) Jørgensen, J. K.; Schöier, F. L.; van Dishoeck, E. F. *Astron. Astrophys.* **2005**, *435*, 177.
(177) Remijian, A. J.; Hollis, J. M. *Astrophys. J.* **2006**, *640*, 842.
(178) Bottinelli, S.; Ceccarelli, C.; Lefloch, B.; Williams, J. P.; Castets, A.; Caux, E.; Cazaux, S.; Maret, S.; Parise, B.; Tielens, A. G. G. M. *Astrophys. J.* **2004**, *615*, 354.
(179) Sakai, N.; Sakai, T.; Yamamoto, S. *Pub. Astron. Soc. Jpn.* **2006**, *58*, 15.
(180) Bottinelli, S.; Ceccarelli, C.; Williams, J. P.; Lefloch, B. *Astron. Astrophys.* **2007**, *463*, 601.
(181) Geppert, W. D.; Hamberg, M.; Thomas, R. D.; Österdahl, F.; Hellberg, F.; Zhaunerchyk, V.; Ehlerding, A.; Millar, T. J.; Roberts, H.; Semaniak, J.; Ugglas, M. Af.; Källberg, A.; Simonsson, A.; Kaminska, M.; Karsson, M. *Faraday Discuss.* **2006**, *133*, 177.
(182) Sakai, N.; Sakai, T.; Hirota, T.; Yamamoto, S. *Astrophys. J.* **2009**, *702*, 1025.
(183) Hassel, G. E.; Herbst, E.; Garrod, R. T. *Astrophys. J.* **2008**, *681*, 1385.
(184) Aikawa, Y.; Wakelam, V.; Garrod, R. T.; Herbst, E. *Astrophys. J.* **2008**, *674*, 993.
(185) Sakai, N.; Sakai, T.; Hirota, T.; Yamamoto, S. *Astrophys. J.* **2010**, *722*, 1633.
(186) Sakai, N.; Yamamoto, S. *Chem. Rev.* **2013**, this volume
(187) Aikawa, Y.; Wakelam, V.; Hersant, F.; Garrod, R. T.; Herbst, E. *Astrophys. J.* **2012**, *760*, 40.
(188) Masunaga, H.; Miyama, S. M.; Inutsuka, S. *Astrophys. J.* **1998**, *495*, 346.
(189) Masunaga, H.; Inutsuka, S. *Astrophys. J.* **2000**, *531*, 350.
(190) Yildiz, U. A.; van Dishoeck, E. F.; Kristensen, L. E.; Visser, R.; Jørgensen, J. K. *Astron. Astrophys.Lett.* **2010**, *521*, 40.
(191) Yildiz, U. A.; Kristensen, L. E.; van Dishoeck, E. F.; Belloche, A.; van Kempen, T. A.; Hogerheijde, M. R.; Güsten, R.; van der Marel, N. *Astron. Astrophys.* **2012**, *542*, 86.
(192) Alonso-Albi, T.; Fuente, A.; Crimier, N.; Caselli, P.; Ceccarelli, C.; Johnston, D.; Planesas, P.; Rizzo, J. R.; Wyrowski, F.; Tafalla, M.; Lefloch, B.; Maret, S.; Dominik, C. *Astron. Astrophys.* **2010**, *518*, 52.
(193) Fuente, A.; Caselli, P.; McCoey, C.; Cernicharo, J.; Johnstone, D.; Fich, M.; van Kempen, T.; van Dishoeck, E. F.; Yildiz, U.; Visser, R.; Kristensen, L.; Alonso-Albi, T.; Herpin, F.; Tisi, S. *Astron. Astrophys.* **2012**, *540*, 75.
(194) Kenyon, S. J.; Hartmann, L. W.; Strom, K. M.; Strom, S. E. *Astron. J.* **1990**, *99*, 869.
(195) Evans, N. J., II; Dunham, M. M.; Jørgensen, J. K.; Enoch, M. L.; Merín, B.; van Dishoeck, E. F.; Alcalá, J. M.; Myers, P. C.; Stapelfeldt, K. R.; Huard, T. L.; Allen, L. E.; Harvey, P. M.; van Kempen, T.; Blake, G. A.; Koerner, D. W.; Mundy, L. G.; Padgett, D. L.; Sargent, A. I. *Astrophys. J. Suppl.* **2009**, *181*, 321.
(196) Kim, H. J.; Evans, N. J., II; Dunham, M. M.; Lee, J. E.; Pontoppidan, K. M. *Astrophys. J.* **2012**, *758*, 38.
(197) Visser, R.; Bergin, E. A. *Astrophys. J. Lett.* **2012**, *754*, 18.
(198) Hidaka, H.; Watanabe, M.; Kouchi, A.; Watanabe, N. *Astrophys. J.* **2009**, *702*, 291.
(199) Taquet, V.; Caccarelli, C.; Kahane, C. *Astrophys. J.* **2012**, *748*, L3.
(200) Parise, B.; Ceccarelli, C.; Tielens, A. G. G. M.; Castets, A.; Caux, E.; Lefloch, B.; Maret, S. *Astron. Astrophys.* **2006**, *453*, 949.
(201) Machida, M. N.; Inutsuka, S.; Matsumoto, T. *Astrophys. J.* **2008**, *676*, 1088.
(202) Ohashi, N.; Hayashi, M.; Ho, P. T. P.; Momose, M.; Tamura, M.; Hirano, N.; Sargent, A. I. *Astrophys. J.* **1997**, *488*, 317.
(203) Tobin, J. J.; Hartmann, L.; Chiang, H.-F.; Wilner, D. J.; Looney, L. W.; Loinard, L.; Calvet, N.; D'Alessio, P. *Nature* **2012**, *492*, 83.
(204) Yen, H. -W.; Takakuwa, S.; Ohashi, N.; Ho, P. T. P. *Astrophys. J.* **2013**, *772*, 22.
(205) Visser, R.; van Dishoeck, E. F.; Doty, S. D.; Dullemond, C. P. *Astron. Astrophys.* **2009**, *495*, 881.
(206) Visser, R.; Doty, S. D.; van Dishoeck, E. F. *Astron. Astrophys.* **2011**, *534*, 132.
(207) Furuya, K.; Aikawa, Y.; Taomida, K.; Matsumoto, T.; Saigo, K.; Tomisaka, K.; Hersant, F.; Wakelam, V. *Astrophys. J.* **2012**, *758*, 86.
(208) Machida, M. N.; Inutsuka, S.; Matsumoto, T. *Astrophys. J.* **2008**, *724*, 1006.
(209) Harsono, D.; Visser, R.; Bruderer, S.; van Dishoeck, E. F.; Kristensen, L. E. *Astron. Astrophys.* **2013**, *555*, 45.
(210) van Weeren, R. J.; Brinch, C.; Hogerheijde, M. R. *Astron. Astrophys.* **2009**, *497*, 773.
(211) Yorke, H. W.; Bodenheimer, P. *Astrophys. J.* **1999**, *525*, 330.
(212) Jørgensen, J. K.; Schöier, F. L.; van Dishoeck, E. F. *Astron. Astrophys.* **2004**, *416*, 603.
(213) Hincelin, U.; Wakelam, V.; Commerçon, B.; Hersant, F.; Guilloteau, S. *Astrophys. J.* **2013**, *775*, 44.
(214) Tomida, K.; Machida, M. N.; Saigo, K.; Tomisaka, K.; Matsumoto, T. *Astrophys. J.* **2010**, *725*, L239.
(215) Commerçon, B.; Launhardt, R.; Dullemond, C.; Henning, T. *Astron. Astrophys.* **2012**, *545*, 98.
(216) Tielens, A. G. G. M.; Hagen, W. *Astron. Astrophys.* **1982**, *114*, 245.
(217) Vasyunin, A.; Herbst, E. *Astrophys. J.* **2013**, *762*, 86.
(218) Cuppen, H. M.; van Dishoeck, E. F.; Herbst, E.; Tielens, A. G. G. M. *Astron. Astrophys.* **2009**, *508*, 275.
(219) Garrod, R. T. *Astron. Astrophys.* **2008**, *491*, 239.
(220) Bacmann, A.; Taquet, V.; Faure, A.; Kahane, C.; Ceccarelli, C. *Astron. Astrophys.* **2012**, *541*, L12.

(221) Vasyunin, A. I.; Herbst, E. *Astrophys. J.* **2013**, *769*, 34.
(222) Yurimoto, H.; Kuramoto, K.; Krot, A. N.; Scott, E. R. D.; Cuzzi, J. N.; Thiemens, M. H.; Lyons, J. R. In *Protostars and Planets V*; Reipurth, B., Jewit, D., Keil, K., Eds.; University of Arizona Press: Tucson, AZ, 2007; p 849.
(223) van Dishoeck, E. F.; Black, J. H. *Astrophys. J.* **1988**, *334*, 771.
(224) Langer, W. D.; Graedel, T. E.; Frerking, M. A.; Armentrout, P. B. *Astrophys. J.* **1984**, *277*, 581.
(225) Langer, W. D.; Graedel, T. E. *Astrophys. J. Suppl.* **1989**, *69*, 241.
(226) Terzieva, R.; Herbst, E. *Mon. Not. R. Astron. Sci.* **2000**, *317*, 563.
(227) Furuya, K.; Aikawa, Y.; Sakai, N.; Yamamoto, S. *Astrophys. J.* **2011**, *731*, 38.
(228) Lee, J. E.; Bergin, E. A.; Lyons, J. R. *Meteorit. Planet. Sci.* **2008**, *43*, 1351.
(229) Wirström, E. S.; Charnley, S. B.; Cordiner, M. A.; Milam, S. *Astrophys. J. Lett.* **2012**, *757*, 11.
(230) Lunine, J. I.; Engel, S.; Rizk, B.; Horanyi, M. *Icarus* **1991**, *94*, 333.
(231) Ilee, J. D.; Boley, A. C.; Caselli, P.; Durisen, R. H.; Hartquist, T. W.; Rawlings, J. M. C. *Mon. Not. R. Astron. Soc.* **2011**, *417*, 2950.
(232) Müller, H. S. P.; Schlöder, F.; Stutzki, J.; Winnewisser, G. *J. Mol. Struct.* **2005**, *742*, 215.
(233) Fortman, S. M.; McMillan, J. P.; Neese, C. F.; Randall, S. K.; Remijan, A. J.; Wilson, T. L.; De Lucia, F. C. *J. Mol. Spectrosc.* **2012**, *280*, 11.
(234) Schöier, F. L.; van der Tak, F. F. S.; van Dishoeck, E. F.; Black, J. H. *Astron. Astrophys.* **2005**, *432*, 369.